The absorption spectrum of nitrous oxide between 8325 and 8622 cm–1

E.V. Karlovets, S. Kassi, S.A. Tashkun, A. Campargue

Journal of Quantitative Spectroscopy and Radiative Transfer

The absorption spectrum of nitrous oxide between 8325 and 8622 cm-1

--Manuscript Draft--

Manuscript Number:	JQSRT-D-20-00055R1
Article Type:	VSI:HITRAN2020
Keywords:	Nitrous oxide, N2O, high-resolution spectra, Cavity Ring Down spectroscopy, line positions, line intensities, HITRAN, HITEMP.
Corresponding Author:	alain Campargue cnrs Saint Martin d'Hères, France
First Author:	Ekatarina Karlovets
Order of Authors:	Ekatarina Karlovets
	Sergey Tashkun
	Samir Kassi
	Alain Campargue
Abstract:	The weak high-resolution absorption spectrum of natural nitrous oxide has been recorded by high sensitivity cavity ring down spectroscopy (CRDS) near 1.18 μm. The frequency scale of the spectra was obtained by coupling the CRDS spectrometer to a self-referenced frequency comb. The room temperature recordings, performed with a pressure of 1 Torr, cover the 8325-8622 cm -1 spectral interval where previous observations were very scarce. More than 3300 lines belonging to four N 2 O isotopologues (14 N 2 16 O, 14 N 15 N 16 O, 15 N 14 N 16 O, and 14 N 2 18 O) are measured . Line intensities at room temperature range between 1.2×10 -25 and 3.8×10 -30 cm/molecule. The rovibrational assignments were obtained by comparison with predictions based on the global modeling of the line positions and intensities performed within the framework of the method of effective operators. The band-by-band analysis led to the determination of the rovibrational parameters of a total of 47 bands. All identified bands belong to the Δ P = 14-16 series of transitions, where P =2 V 1 + V 2 +4 V 3 is the polyad number (V i= 1-3 are the vibrational quantum numbers). Among these bands, only five were previously observed and bands of the Δ P = 15 series are reported for the first time. The position and intensity comparisons to the HITRAN2016 and HITEMP2019 spectroscopic databases are discussed. The HITRAN line list is limited to only four (calculated) bands of the 14 N 2 18 O isotopologue in the studied region while Δ P = 15 bands are missing in the HITEMP list. The present work will help to improve future versions of the spectroscopic databases of nitrous oxide, a strong greenhouse gas.
Suggested Reviewers:	Valery Perevalov vip@iao.ru
	Yan Tan Tanyan0921@hotmail.com Has worked on N2O at USTC in the group of Prof. Hu
	David Jacquemart david.jacquemart@upmc.fr
Response to Reviewers:	

Dear Sir,
Please find attached the revised version of our paper:

The absorption spectrum of nitrous oxide between 8325 and 8622 cm-1

by E.V. Karlovets, S.Kassi, S.A.Tashkun and A. Campargue

that we submit to the HITRAN2020 SI of JQSRT.

We hope that the amended version is now suitable for publication in JQSRT.
Regards
Alain Campargue

Response to the reviewers

Ref: JQSRT-D-20-00055

The absorption spectrum of nitrous oxide between 8325 and 8622 cm^{-1}

by E. Karlovets, S. Kassi, S. Tashkun A. Campargue

We thank the two reviewers for their useful comments which were taken into account as detailed below.

Reviewer #1: Good work, see attached file.

The manuscript is dealing with the analysis of a single experimental spectrum and the retrieval of line positions and intensities for several bands belonging to 4 isotopologues of N_2O. CRDS set up is used with a flow of N_2O commercial sample regulated at 1 Torr allowing to access to very weak absorption transitions. In addition to numerous new measurements (more than 3000 in total), the authors produced spectroscopic parameters of levels involved in measured transitions. Measurements and comparisons with calculations are available as supplementary material. Comparisons with HITRAN and HITEMP are given showing the lack of spectroscopic data in databases.

Improvements of the spectroscopic knowledge of N_2O molecule has been achieved through this work. The manuscript is well written and totally suitable for the Journal of Quantitative Spectroscopy and Radiative Transfer. Some few minor comments/corrections exposed below:

1/ In Figure 7 and graphical abstract, a typo is probably present for legend of green symbols ($^{14}N_2{}^{18}O$ instead of $^{14}N_2{}^{16}O$). I guessed it by seeing Figs. 3 and 4 (you are using green for this isotopologue). I checked also HITRAN, and there is no transition of $^{14}N_2{}^{16}O$ after 7800 cm-1 so that green symbol from Fig 7 cannot be main isotopologue transitions.

Thank you for pointing this typo. The green symbols should correspond to $^{14}N_2{}^{18}O$. $^{14}N_2{}^{16}O$ transitions are plotted with black symbols. It is now corrected.

2/ The authors wrote that the measured intensities are given in natural abundance, that the sample is almost pure. But I supposed you assumed the commercial sample to be in natural abundance to derive line intensities. This should be clarified in the text.

Yes, the reviewer is right. We cannot be sure that the isotopologue abundance in our sample coincide with HITRAN abundance values. The sentence "*The line intensities of all nitrous oxide isotopologues are given at 296 K and correspond to the natural abundance."* has been modified: *"The line intensities of all nitrous oxide isotopologues are given at 296 K. The isotopic abundance of the used commercial N_2O sample is assumed to be close to the "natural" abundance adopted in the HITRAN database for the different N_2O isotopologues (see* ***Table 1****)."*

We have also added as a comment of Fig. 5:

"Let us mention that the intensity comparison displayed on ***Fig. 5*** *assumes that the isotopic abundances of the minor isotopologues in our sample coincide to HITRAN values. Small deviations from HITRAN isotopic abundances cannot be excluded and may contribute to small systematic deviations as noted for the intensity of the strongest bands of $^{14}N^{15}N^{16}O$ and $^{15}N^{14}N^{16}O$."*

3/ In sup data, the measured line intensities are given at 296 K whereas temperature of exp spectrum is slightly different. Did you perform temperature conversion for measured line intensities? if yes with which partition function? This should be clarified in the text.

The reviewer is right: the intensities listed in the sup mat were not converted to 296 K and correspond in fact to the recording temperatures which evolved in the 293.8- 294.7 K range. The difference is mostly negligible for cold bands but might be significant for part of the hot bands.

In the revised version of the sup mat, we now indicate: "Meas Int - measured intensities (in cm/molecule) at the recording temperature of 294.2+/-0.5 K."

4/ Results of the fitted EDM parameters for DP=15 should be given in the text.

We have changed the following portion of the text and provide now the *ΔP= 15 EDM parameter values*:

Previous version:

For the purpose of the present analysis, two main ΔP= 15 EDM parameters, namely, $M_{1,1,3,1}$ and $M_{-1,4,1,1}$. (see Ref. [35] for definitions and notations) were determined in the present work. First, on the basis of line positions, the 1113-0000 band of $^{14}N_2\,^{16}O$ belonging to the ΔP= 15 series were assigned in the CRDS spectrum. The values of the $M_{1,1,3,1}$ and $M_{-1,4,1,1}$ parameters were fitted to the corresponding measured intensities.

New version:

For the purpose of the present analysis, two main ΔP= 15 EDM parameters, namely, $M_{0,3,3,1}$ and $M_{3,1,2,1}$ (see Ref. [35] for definitions and notations) were determined in the present work. First, on the basis of line positions, the 1113-0000 and 3112-0000 bands of $^{14}N_2{}^{16}O$ belonging to the ΔP= 15 series were assigned in the CRDS spectrum. The values of the $M_{0,3,3,1}$ and $M_{3,1,2,1}$ parameters were fitted to the corresponding measured intensities. The fitted values are 1.364(6) 10^{-6} Debye and 5.11(6) 10^{-7} Debye, respectively.

Details:

1/ In Figs 8 and 9, the use of green color for $^{14}N_2{}^{18}O$ would be more consistent with Figs. 3 and 4.

It is right, we have changed the color as suggested.

2/In conclusion the authors wrote:

"The high sensitivity absorption spectrum of natural nitrous oxide has been analyzed by CRDS in the 8325-8622 cm-1 range corresponding …"

I believe an high sensitivity absorption spectrum can be recorded by CRDS but "analyzed by CRDS" sounds strange to me. A spectrum can be analyzed by fitting profile programs In the same idea, transitions are not measured (see end of section 1)

"In the present work, more than 3300 transitions belonging to 47 bands of 14N216O, 14N15N16O,15N14N16O, and 14N218O isotopologues were measured and assigned in the…"

Transitions can be assigned and fitted. Or transitions are assigned and line positions and intensities are measured.

We agree with the reviewer:

We now us "recorded" instead of "analyzed" : *The high sensitivity absorption spectrum of natural nitrous oxide has been **recorded** by CRDS in the 8325-8622 cm^{-1} range corresponding to a weak absorption region where previous measurements were very limited. "*

And at the end of Section 1, we deleted "measured":

In the present work, more than 3300 transitions belonging to 47 bands of 14N216O, 14N15N16O,15N14N16O, and 14N218O isotopologues were ~~measured and~~ assigned in the…"

Reviewer #2: Manuscript JQSRT-D-20-00055 titled "The absorption spectrum of nitrous oxide between 8325 and 8622 cm-1" reports the continuous-wave cavity ring-down spectroscopy of a natural sample of N2O over a broad infrared bandwidth of ~300 cm-1. The data for several isotopocules of N2O fills a missing data gap present in HITRAN2016. The newly reported reference data includes the assignment of dozens of band not previously reported, and therefore is highly appropriate for JQSRT. The description of experimental techniques and spectral analysis is sufficient, and citations of the necessary references are appropriate. I recommend that the authors contemplate the below list of minor comments:

Highlight #2: "More than 3300 lines of 47 bands of ..."

Corrected

Page 3, paragraph 2, line 1: "Concerning the spectroscopy of nitrous oxide ..."

Corrected

Page 3, paragraph 2, line 7: "This spectral range was investigated using a series of about ..."

Corrected

Page 4, Experimental details, line 4: An abbreviation for self-referenced frequency comb was already introduced on page 3 as SSRFC. Please be consistent.

In fact, we speak about self-referenced frequency comb only twice and the abbreviation is in fact useless. It has been deleted.

Page 4, Experimental details, line 7: was the spectral resolution of 1.3E-3 cm-1 equal to the cavity free spectral range? Please verify.

In fact, the 1.3E-3 cm-1 value corresponds to the step of the sampling that we chose. It could be even smaller but this would increase the recording time. This value is not related to the FSR which is 3.57 E-3 cm-1 for our cavity length of 140 cm. Note that our cavity is not frequency-stabilized and the ring-down events occur in case of accidental coincidence between the frequency of the laser and that of a longitudinal mode of the cavity.

Page 6, beginning after Eq. (1): various mathematical symbols on page 6 did not convert to PDF. Please correct.

It is now Ok on our pdf

We hope that the amended version is now suitable for publication in JQSRT.

Highlights

- High sensitivity CRDS of the weak absorption spectrum of N_2O between the 8325-8622 cm^{-1}
- More than 3300 of 47 bands of $^{14}N_2{}^{16}O$, $^{14}N^{15}N^{16}O$, $^{15}N^{14}N^{16}O$, and $^{14}N_2{}^{18}O$ are measured
- Only five bands were previously reported, with no intensity information
- Bands corresponding to a $\Delta P = 15$ variation of the polyad number are reported for the first time.
- In the considered region, the HITRAN and HITEMP databases show deficiencies in terms of completeness and accuracy

Graphical Abstract

Click here to access/download;Graphical Abstract;rev_graph_abstract.jpg

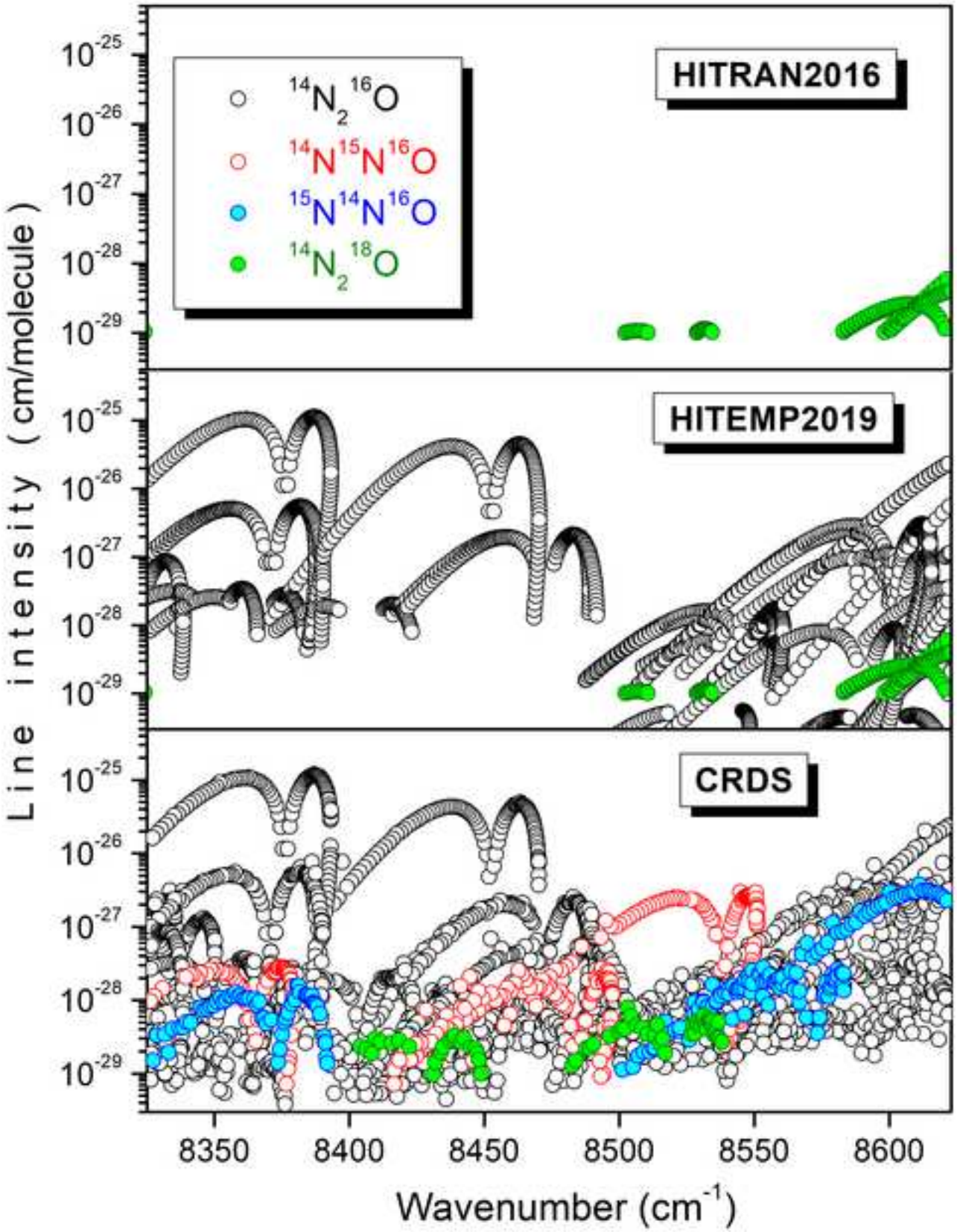

The absorption spectrum of nitrous oxide between 8325 and 8622 cm^{-1}

E.V. Karlovets [1,2*], S. Kassi [3], S.A. Tashkun [4,5] and A. Campargue [3*]

[1] *Harvard-Smithsonian Center for Astrophysics, Atomic and Molecular Physics Division, 60 Garden St, Cambridge, MA, USA*
[2] *Tomsk State University, Laboratory of Quantum Mechanics of Molecules and Radiative Processes, 36, Lenin Avenue, 634050, Tomsk, Russia*
[3] *Univ. Grenoble Alpes, CNRS, LIPhy, 38000 Grenoble, France*
[4] *V.E. Zuev Institute of Atmospheric Optics, 1, Academician Zuev square, 634055 Tomsk, Russia*
[5] *Ural Federal University, Climate and Environmental Physics Laboratory, 19, Mira Avenue, 620002 Yekaterinburg, Russia*

Number of pages: 24 30 December 2020

Number of tables: 4

Number of figures: 9

Keywords: Nitrous oxide, N_2O, high-resolution spectra, Cavity Ring Down spectroscopy, line positions, line intensities, HITRAN, HITEMP.

* Corresponding authors:
E-mails: alain.campargue@univ-grenoble-alpes.fr (A. Campargue),
ekaterina.karlovets@cfa.harvard.edu (E.V. Karlovets)

Abstract

The weak high-resolution absorption spectrum of natural nitrous oxide has been recorded by high sensitivity cavity ring down spectroscopy (CRDS) near 1.18 μm. The frequency scale of the spectra was obtained by coupling the CRDS spectrometer to a self-referenced frequency comb. The room temperature recordings, performed with a pressure of 1 Torr, cover the 8325-8622 cm^{-1} spectral interval where previous observations were very scarce. More than 3300 lines belonging to four N_2O isotopologues ($^{14}N_2{}^{16}O$, $^{14}N^{15}N^{16}O$, $^{15}N^{14}N^{16}O$, and $^{14}N_2{}^{18}O$) are measured with a position accuracy better than 1×10^{-3} cm^{-1} for most of the lines. Line intensities at room temperature range between 1.2×10^{-25} and 3.8×10^{-30} cm/molecule. The rovibrational assignments were obtained by comparison with predictions based on the global modeling of the line positions and intensities performed within the framework of the method of effective operators. The band-by-band analysis led to the determination of the rovibrational parameters of a total of 47 bands. All identified bands belong to the ΔP= 14-16 series of transitions, where $P=2V_1+V_2+4V_3$ is the polyad number ($V_{i=1-3}$ are the vibrational quantum numbers). Among these bands, only five were previously observed and bands of the ΔP= 15 series are reported for the first time. Local resonance perturbations affecting two bands are identified and analyzed. The position and intensity comparisons to the HITRAN2016 and HITEMP2019 spectroscopic databases are discussed. The HITRAN line list is limited to only four (calculated) bands of the $^{14}N_2{}^{18}O$ isotopologue in the studied region while ΔP= 15 bands are missing in the HITEMP list. The present work will help to improve future versions of the spectroscopic databases of nitrous oxide, a strong greenhouse gas.

1. Introduction

Nitrous oxide (N_2O) is a highly efficient greenhouse gas which plays an important role in the destruction of stratospheric ozone. It is also naturally present in the atmosphere as part of the Earth's nitrogen cycle, and has a variety of natural and anthropological sources. Nitrous oxide is emitted by agricultural activities (~75% of the total emissions), combustion of fossil fuels and solid waste, as well as by the treatment of wastewater. Atmospheric nitrous oxide has a strong warming effect power, typically 300 times stronger than carbon dioxide, both having a similar atmospheric lifetime of about one century. The N_2O atmospheric concentration of about 330 ppb is increasing at a rate of about 1 ppb/year.

Concerning the spectroscopy of nitrous oxide, the recent exhaustive review by Tashkun [1] indicates that about 61500 absorption and emission lines of the main isotopologue, $^{14}N_2{}^{16}O$, have been reported in the literature below 15000 cm^{-1}. Most of the data were obtained by Fourier transform spectroscopy (FTS) (*e.g.* Refs. [2-7]), cavity ring down spectroscopy (CRDS) (*e.g.* Refs. [8-14]), and intracavity laser absorption spectroscopy (ICLAS) (*e.g.* Refs. [15-21]). The series of our previous CRDS investigations [8-14,22,23] covered the 5696 -8332 cm^{-1} near-infrared region and provided a total of about 19000 $^{14}N_2{}^{16}O$ line positions. This spectral range was investigated using a series of f about one hundred fibered distributed feedback (DFB) lasers were previously used as light source below 7920 cm^{-1} [8-11,14,22,23] and an external cavity diode laser (ECDL) was adopted in the of 7915–8334 cm^{-1} study [12,13]. ECDLs allow for a more efficient light injection into the CRDS cell and thus an improved sensitivity. The present investigation in the 8325-8622 cm^{-1} spectral interval used also an ECDL as light source. In addition, the CRD spectrometer is coupled to a self-referenced frequency comb providing accurate frequency value for each ring down event. As a result, the achieved sensitivity of the spectra (noise equivalent absorption α_{min}~ 10^{-12} cm^{-1}) allowed for using a pressure value limited to 1.0 Torr for the recordings.

Very scarce previous observations are available in the investigated region. They are limited to FTS measurements of three bands of $^{14}N_2{}^{16}O$ [15,16], two bands of $^{14}N^{15}N^{16}O$ [24] and one band of $^{15}N^{14}N^{16}O$ [25]. Note that the $^{14}N^{15}N^{16}O$ and $^{15}N^{14}N^{16}O$ FTS studies were performed with highly enriched isotopic samples [24,25]. The present sensitivity of the CRDS spectra of natural N_2O allowed extending the observation of these two minor isotopologues in spite of a natural isotopic abundance on the order of 3.6×10^{-3} in the CRDS sample.

In the CRDS study of the 7915- 8334 cm^{-1} interval [12,13], just below the presently studied region, CRDS intensity values together with literature data were used to improve the line intensity modeling of the $^{14}N_2{}^{16}O$ isotopologue. In addition, a global modeling of the line positions of the $^{14}N_2{}^{18}O$ minor isotopologue was performed [13]. As a result, the $^{14}N_2{}^{18}O$ line list was generated and has been adopted for the HITRAN2016 spectroscopic database [26]. Taking into account the small natural

isotopic abundance of $^{14}N_2{}^{18}O$ (1.986×10^{-3}) and the incompleteness of the HITRAN2016 line list for the most abundant isotopologues ($^{14}N_2{}^{16}O$, $^{14}N^{15}N^{16}O$, $^{15}N^{14}N^{16}O$), it leads to an unsatisfactory situation of the HITRAN2016 line list which provide many very weak bands of $^{14}N_2{}^{18}O$ while much stronger bands of the main isotopologue are absent. This is the case in the presently studied interval where the HITRAN list is limited to 130 transitions of four bands of $^{14}N_2{}^{18}O$ while most of the absorption is due to the main isotopologue (see below).

In the present work, more than 3300 transitions belonging to 47 bands of $^{14}N_2{}^{16}O$, $^{14}N^{15}N^{16}O$, $^{15}N^{14}N^{16}O$, and $^{14}N_2{}^{18}O$ isotopologues were assigned in the 8325-8622 cm^{-1} spectral interval. The rovibrational assignments were performed with the help of the predictions of the polyad and non-polyad models of effective Hamiltonian described in Refs. [1, 13, 27, 28]. All the bands observed in the presently investigated region correspond to ΔP= 14 and 16 variations of the polyad quantum numbers except for three bands of $^{14}N_2{}^{16}O$ corresponding to ΔP= 15 which are the first ones detected for this series ($P= 2V_1+V_2+4V_3$ is the polyad number, $V_{i=1-3}$ being the vibrational quantum numbers). This paper is organized as follows. The experimental setup and the construction of the measured lists are briefly described in Section 2. In Section 3, we present the detailed data analysis, including the rovibrational assignments and band-by-band analysis, which consists of the fitting of G_v, B_v. D_v, and H_v band parameters and identification of resonance perturbations for $^{14}N_2{}^{16}O$ isotopologue. In Section 4, we discuss the comparison with the spectroscopic list of nitrous oxide: provided in the HITRAN [3] and HITEMP [9] databases.

2. Experimental details

The reader is referred to Refs. [29-33] for the description of the cavity ring down spectrometer and the frequency tuning of the ECDL. The accurate frequency value associated to each ring-down event was obtained by using a Fizeau type wavemeter (High Finesse WS-U-30 IR) and a self-referenced frequency comb, providing sub-100 kHz accuracy to the instantaneous frequency readings [33]. Mode-hop-free tuning range of up to 1.3 cm^{-1} could be obtained (see Ref. [12] for details). The broadband spectra covering the 8325-8622 cm^{-1} range were obtained by concatenation of a series of partly overlapping, 1.1 cm^{-1} wide individual spectra, recorded with about 1.3×10^{-3} cm^{-1} step sampling, to be compared to the N_2O Doppler line width of about 7×10^{-3} cm^{-1} (HWHM) in the considered region. Each baseline point was obtained by averaging 40 individual events. **Fig. 1** illustrates the sensitivity and high dynamical range on the intensity scale. The noise equivalent absorption evaluated as the *rms* of the baseline fluctuations is around 5×10^{-12} cm^{-1}. A number of interfering lines of water vapor (with relative concentration of about 0.1 %) are observed superimposed on the N_2O spectrum.

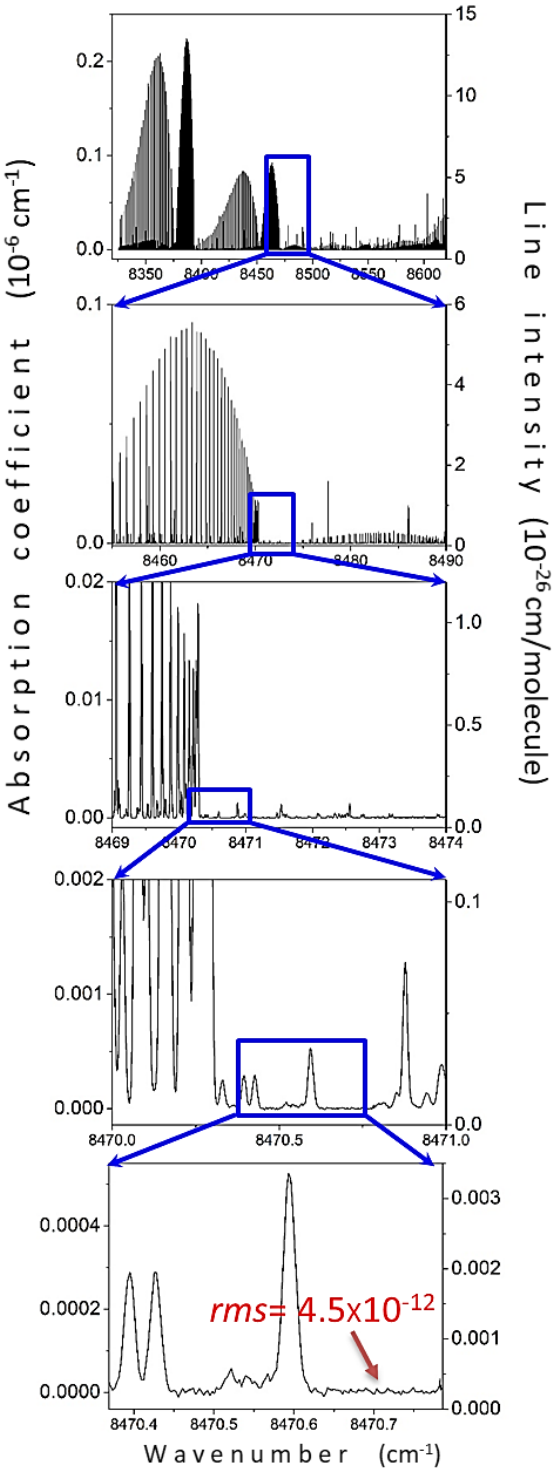

Fig. 1.

CRDS spectrum of nitrous oxide recorded at a pressure of 1.0 Torr. The overview of the entire region presently investigated from 8325 and 8622 cm^{-1} is presented on the upper panel. The right-hand intensity scale is adjusted to correspond approximately to the peak heights. The enlargements illustrate the dynamics achieved on the intensity scale and the noise equivalent absorption ($\alpha_{min} \approx 5\times10^{-12}$ cm^{-1}). The spectrum includes a number of interfering lines due to water vapor present in the CRDS cell as an impurity.

The spectra were recorded in flow regime in order to decrease the impact of the lines of water

vapor degassing from the cell walls. The flow of nitrous oxide (Alphagaz 99.99% stated purity) was roughly adjusted to 1 sccm with a downstream manual needle valve and the pressure was actively regulated at 1.00 Torr. The temperature of the outer wall of the stainless steel gas cell was monitored with a PT 1000 resistive probe. Over the whole spectrum recordings, the temperature evolved in the 293.8- 294.7 K range.

The line centers and intensities were determined using an interactive least squares multi-lines fitting program written in LabVIEW. The line profile was assumed to be of Voigt type. The line position, integrated absorbance, Lorentzian widths and the corresponding local baseline (assumed to be a linear function of the wavenumber) were provided by the fitting procedure. The HWHM of the Gaussian component was fixed to the theoretical value of the Doppler width of the considered nitrous oxide isotopologue. **Fig. 2** illustrates the quality of the spectrum fit near 8329.4 cm^{-1}.

The line intensity, S_{v_0} (cm/molecule), of a rovibrational transition centered at v_0, was obtained from the integrated absorption coefficient, $A_{v_0}(T)$ (cm^{-2}):

$$A_{v_0}(T) = \int_{line} \alpha_v dv = S_{v_0}(T) N \qquad (1)$$

where v is the wavenumber in cm^{-1}, α_v ıs the absorption is the absorption coefficient in cm^{-1} obtained from the cavity ring down time, τ (in s): $\alpha = \frac{1}{c}\left(\frac{1}{\tau} - \frac{1}{\tau_0}\right)$ where *c* is the light velocity and τ_0 is the ring-down time of the empty cavity, *N* is the molecular concentration in molecule/cm^3 obtained from the measured pressure (*P*) and temperature (*T*) values: *P* = *NkT*. (*k*= 1.38065×10^{-16} erg/K is the Boltzmann constant).

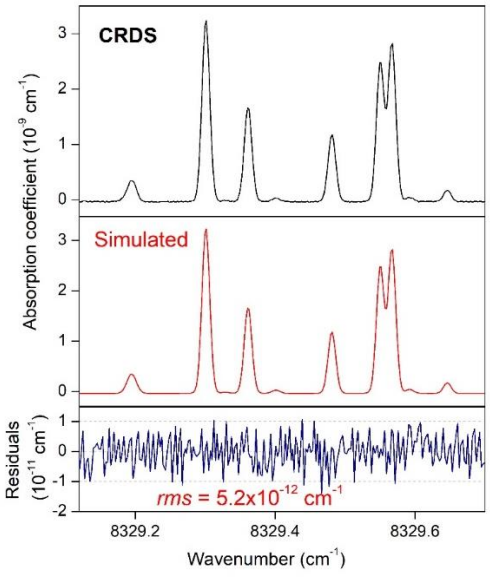

Fig. 2
Fragment of the CRDS and simulated N_2O spectra recorded at 1.0 Torr near 8329.4 cm^{-1}.

3. Rovibrational analysis

3.1. Vibrational assignment

In N_2O, due to the $\omega_3 \approx 2\omega_1 \approx 4\omega_2$ approximate relations between the harmonic frequencies, vibrational states are grouped into polyads characterized by the quantum number $P = 2V_1+V_2+4V_3$. The resulting vibrational energy levels are labeled using the triplet (P, l_2, i) where l_2 is the vibrational angular momentum associated to the bending vibration v_2, and i is the index increasing with the energy. The measured N_2O transitions were assigned with the help of the predictions of the polyad and non-polyad models of effective Hamiltonian (EH) [1,13,27,28]. Up to the recent work of Ref. [1], all the global fittings of the N_2O line positions included only intrapolyad resonance interactions $\Delta P = 0$ (up to the sixth order) but different experimental results made clear that interpolyad interactions, in particular, interpolyad Coriolis interactions are necessary to account for some observed perturbations (see e.g. Refs. [9,12,14,18]). The non-polyad model of the effective Hamiltonian recently developed for the main isotopologue [1], takes into account three types of interpolyad interactions allowing for the coupling between the vibrational states belonging to polyads with ΔP = 1 or 2. The N_2O predicted line lists used for the assignments, contain calculated line positions and intensities for the four most abundant isotopologues of N_2O: $^{14}N_2{}^{16}O$ (446), $^{14}N^{15}N^{16}O$ (456), $^{15}N^{14}N^{16}O$ (546), and $^{14}N_2{}^{18}O$ (448). The line positions of $^{14}N_2{}^{16}O$ were calculated using non-polyad model of effective Hamiltonian [1]. The line positions of $^{14}N^{15}N^{16}O$, $^{15}N^{14}N^{16}O$, and $^{14}N_2{}^{18}O$ were calculated using the polyad models of effective Hamiltonian [13, 28]. The line lists were computed assuming a temperature of 296 K and an intensity cut off 10^{-30} cm/molecule for nitrous oxide in natural abundance.

The line intensities were calculated using the effective dipole moment model [6,13]. All identified bands belong to the ΔP= 14-16 series of transitions. For the ΔP= 14 and 16 series of transitions of $^{14}N_2{}^{16}O$ effective dipole moment parameters were taken from Ref. [6]. These parameters were also used to compute the intensities of other isotopologues. The rationale for this approach is that the main effective dipole moment (EDM) parameters slightly depend on the isotopologue masses. This fact was demonstrated both for symmetric and asymmetric isotopologues of CO_2 [34].

The ΔP= 15 series of transitions contribute to the absorption in our region but, in absence of previous intensity information, no EDM parameters were determined for this series, up to now. For the purpose of the present analysis, two main ΔP= 15 EDM parameters, namely, $M_{0,3,3,1}$ and $M_{3,1,2,1}$ (see Ref. [35] for definitions and notations) were determined in the present work. First, on the basis of line positions, the 1113-0000 and 3112-0000 bands of $^{14}N_2{}^{16}O$ belonging to the ΔP= 15 series were assigned in the CRDS spectrum. The values of the $M_{0,3,3,1}$ and $M_{3,1,2,1}$ parameters were fitted to the corresponding measured intensities. The fitted values are 1.364(6) 10^{-6} and 5.11(6) 10^{-7} Debye, respectively. All line intensities were then calculated with the polyad models of effective Hamiltonian [13,27,28]. At the

final stage of the line list calculations, the $^{14}N_2{}^{16}O$ line positions were replaced with those calculated using the non-polyad EH model [1].

Finally, a total of 3307 lines belonging to 47 bands of the $^{14}N_2{}^{16}O$, $^{14}N^{15}N^{16}O$, $^{15}N^{14}N^{16}O$, and $^{14}N_2{}^{18}O$ isotopologues were assigned (see **Table 1**). An overview of the assigned lines is presented in **Fig. 3** while the list of observed bands is given in **Table 2.** Line intensities range between 1.0×10^{-25} and 3.8×10^{-30} cm/molecule. Only five of the reported bands were previously observed [15,16,24,25], all by FTS (see **Tables 1 and 2)**. Eight bands belong to the minor isotopologues. They include the most excited bands of the $^{14}N_2{}^{18}O$ isotopologue observed so far. Note that none of the previous FTS studies provided intensity information in the region.

Table 1
Summary of the number of transitions and bands of the different N_2O isotopologues assigned in this work by CRDS in the 8325 and 8622 cm^{-1} region.

Isotopologue	Abundance [26]	Number of bands [a]	Number of transitions
$^{14}N_2{}^{16}O$	0.9903	39/2 [12,13]	2745
$^{14}N^{15}N^{16}O$	3.641×10^{-3}	3/2 [24]	299
$^{15}N^{14}N^{16}O$	3.641×10^{-3}	3/1 [25]	199
$^{14}N_2{}^{18}O$	1.986×10^{-3}	2/0	64
Total	1.0	47 (5)	3307

Note:
[a] The second number is the number of bands previously observed in the literature in the studied region with corresponding reference.

The complete N_2O line list, including the isotopologue identification, rovibrational assignments, line parameters observed in the present work and calculated positions and intensities is provided as supplementary material. The line intensities of all nitrous oxide isotopologues are given at 296 K. The isotopic abundance of the used commercial N_2O sample is assumed to be close to the "natural" abundance adopted in the HITRAN database for the different N_2O isotopologues (see **Table 1**).

Note that the recorded spectrum includes 877 water lines which were identified by comparison to the HITRAN2016 spectroscopic database [26]. At the final stage of the analysis, about 680 lines, mostly very weak remained unassigned.

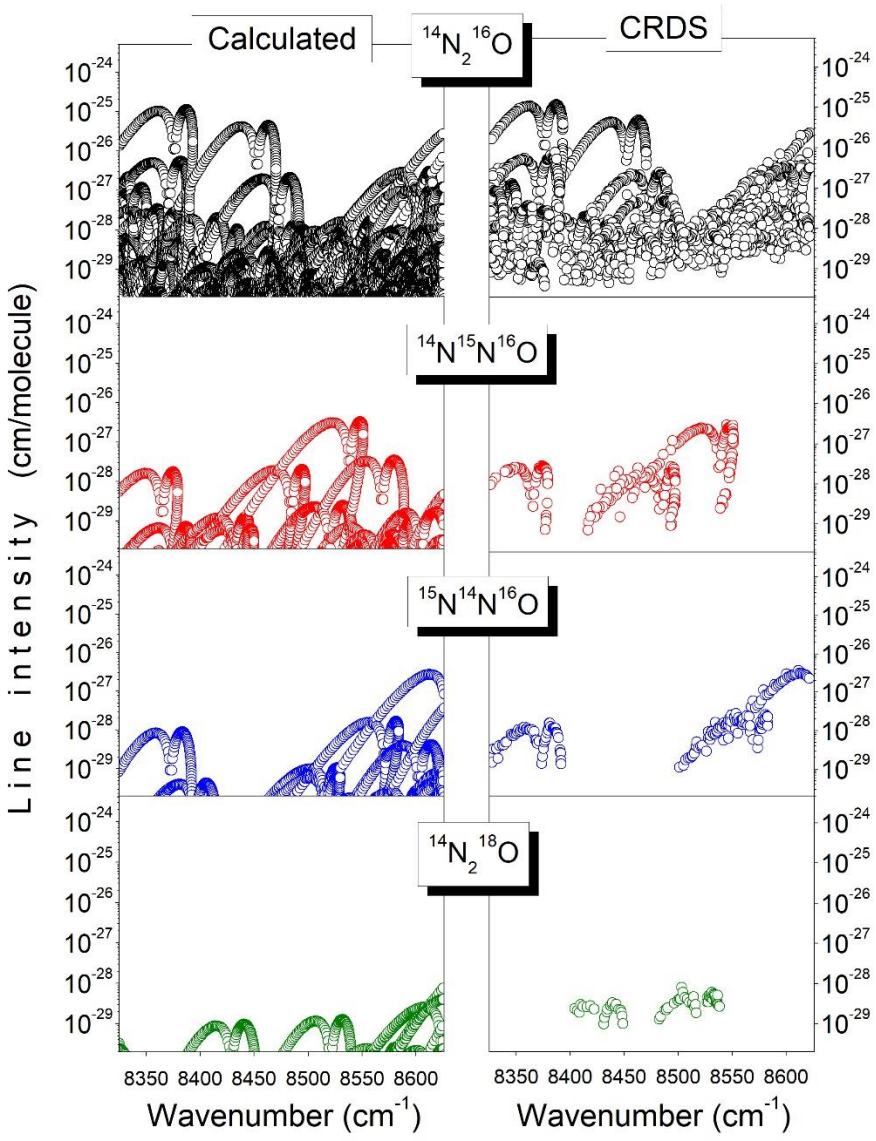

Fig.3.
Overview comparison between the CRDS observations in the 8325-8622 cm^{-1} spectral region and the predictions within the framework of the method of effective operators [1,6,27,28] for the four N_2O isotopologues contributing to the spectrum.

An overview comparison of the differences between the measured line positions and their predicted values [1,13,28] are plotted *versus* the wavenumber in **Fig. 4**. The $^{14}N_2{}^{16}O$, $^{14}N^{15}N^{16}O$ and $^{15}N^{14}N^{16}O$ line positions shows deviations limited to 0.048 cm^{-1}. In the case of the $^{14}N_2{}^{18}O$ isotopologue, deviations increase up to 0.43 cm^{-1}.

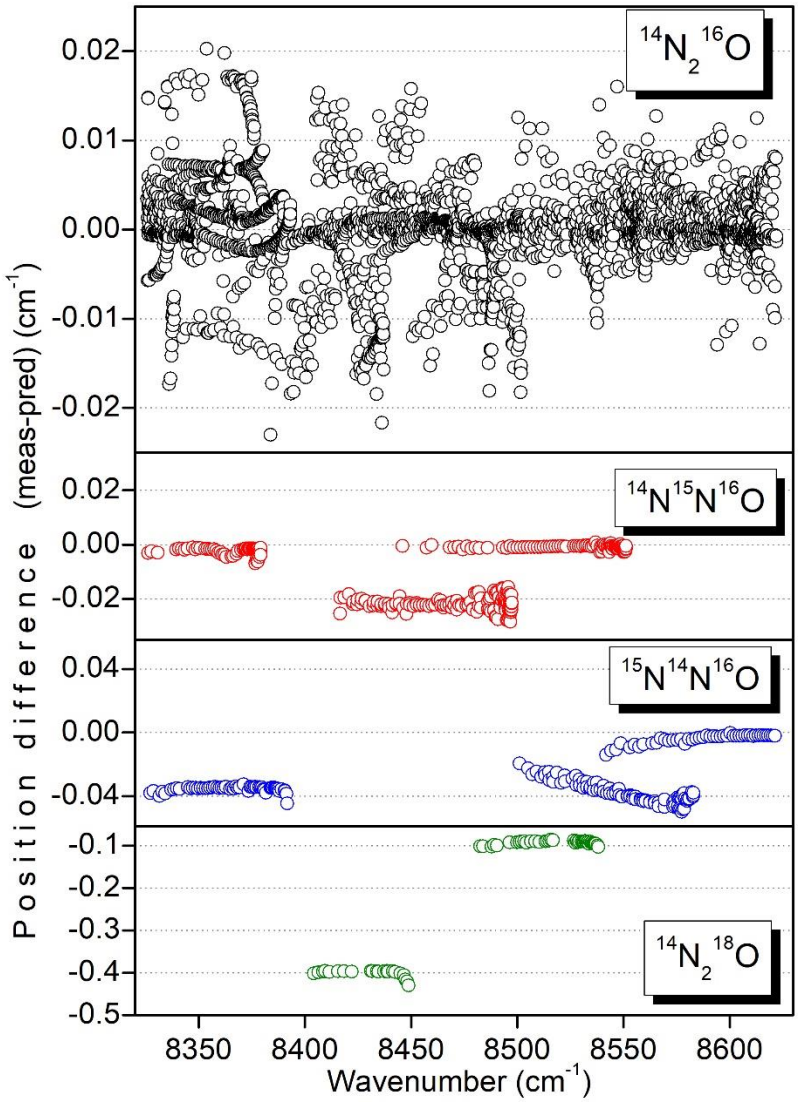

Fig. 4
Differences between the line positions predicted using the effective Hamiltonians and the measured values, for the first four N_2O isotopologues. The line positions of $^{14}N_2{}^{16}O$ were calculated using non-polyad model of effective Hamiltonian [1] while those of the minor isotopologues were obtained using the polyad models of effective Hamiltonian [13, 28].

Fig. 5 presents the comparison between the experimental intensities and their calculated values computed using the ΔP= 14-16 EDM parameters. We estimate that the accuracy of our measured line intensities to be 3% or better for most lines and up to 20% for the weakest or strongly blended lines. As can be seen by **Fig. 5**, the intensity ratios vary roughly from 0.7 to 2 for the $^{14}N^{15}N^{16}O$ and $^{15}N^{14}N^{16}O$ isotopologues. In the case of the $^{14}N_2{}^{16}O$ and $^{14}N_2{}^{18}O$ isotopologues, calculated intensities of some lines are underestimated by a factor up to 4. In general, the calculated intensities are smaller than observed. This may indicate that the set of EDM parameters of the ΔP= 14 and 16 series which were derived from a fit of a limited set of relatively strong bands measured by FTS [6] are missing some important EDM parameters. Considering the importance of the observed deviations, the

present line intensity measurements will be useful to improve the EDM parameters of the Δ*P*= 14 and 16 series of transitions. Let us mention that the intensity comparison displayed on **Fig. 5** assumes that the isotopic abundances of the minor isotopologues in our sample coincide to HITRAN values. Small deviations from HITRAN isotopic abundances cannot be excluded and may contribute to small systematic deviations as noted for the intensity of the strongest bands of $^{14}N^{15}N^{16}O$ and $^{15}N^{14}N^{16}O$.

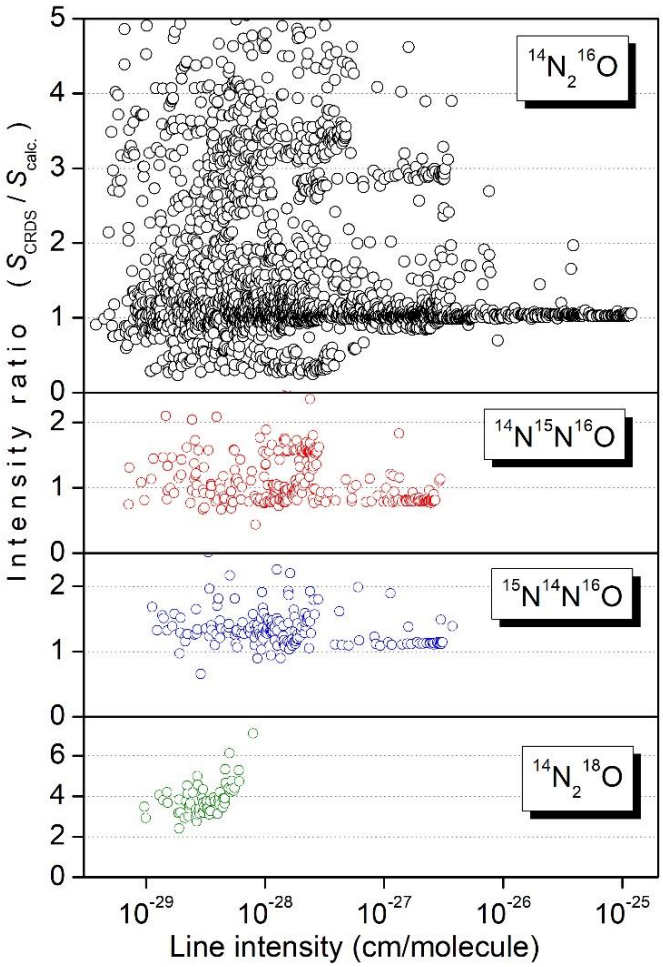

Fig. 5. Ratios of the N_2O line intensities measured by CRDS to those predicted using the effective operator approach in the 8325-8622 cm^{-1} spectral region.

3.2. Spectroscopic analysis of the line positions and rovibrational perturbations

The standard expression of the vibration–rotation energy levels was used for the band-by-band fit of the spectroscopic parameters:

$$F_v(J) = G_v + B_v J(J+1) - D_v J^2(J+1)^2 + H_v J^3(J+1)^3 \quad (1)$$

where G_v is the vibrational term value, B_v is the rotational constant, D_v and H_v are the centrifugal distortion constants, J is the angular momentum quantum number.

In the case of hot bands involving *e* and *f* rotational levels, the *ee*, *ef*, *fe*, and *ff* sub-bands were considered independently. The lower state constants were constrained to the values obtained by Toth [4,5]. Spectroscopic parameters of 67 upper vibrational levels of a total of 47 bands were derived from

standard band-by-band fits to the measured line positions. **Table 2** lists the obtained constants of the different N_2O bands ordered in increasing wavenumber of their band center. The typical *rms* values of the fits are better than 1×10^{-3} cm^{-1}. The observation of hot bands arising from *P*= 1-3 lower states gives access to the upper levels belonging to the *P*= 14-20 polyads. The most excited level observed is the 0005e upper level of $^{14}N_2{}^{16}O$ near 10815 cm^{-1} observed through the $5\nu_3$-ν_3 hot band centered near 8591.5 cm^{-1}. The results of the band-by-band fit of the spectroscopic parameters are provided as supplementary material. This archive file includes for each band, spectroscopic parameters of the lower state fixed to the literature values, observed and calculated line positions, fitted spectroscopic parameters of the upper state, errors on the fitted parameters (in % and in cm^{-1}) and *rms* value of the fit.

During the fitting of the spectroscopic constants, we found that two bands were perturbed. The characteristics of the interaction mechanism identified on the basis of the effective Hamiltonian model are summarised in **Table 3.**

Table 3
Summary of the local resonance interactions of $^{14}N_2{}^{16}O$ bands between 8325 and 8622 cm^{-1}.

Perturbed band	Center (cm^{-1})	Upper state ($P\ l_2\ i$)	G_v	Resonance interaction mechanism	J_{cross}
6001e-1000e	8321.43080	(16 0 19)	9606.334	Intrapolyad anharmonic interaction (16 0 19)↔(16 0 18)	29
1004e-1000e	8603.66425	(18 0 4)	9888.568	Intrapolyad anharmonic interaction (18 0 4) ↔(18 0 3)	14
				Interpolyad Coriolis interaction (18 0 4) ↔(17 1 10)	34

The 6001e-1000e band at 8321.4 cm^{-1} reaching the ($P\ l_2\ i$)= (16 0 19) upper state is perturbed around the energy crossing at *J*= 29 by an anharmonic resonance interaction with the (16 0 18) perturber state belonging to the same *P*= 16 polyad. The perturbation induces shifts of the line positions up to 0.02 cm^{-1} around the energy crossing at *J*= 29. Let us mention that the vibrational eigenfunction of the (16 0 18) perturber state is highly delocalized and has a maximum fraction of only 25% for the $(v_1\ v_2 l_2 v_3)$ = (0 16 0 0) normal mode pure bending state. As a further example of the ambiguity of the normal mode vibrational labelling, let us note that the band centered near 8349.74 cm^{-1} labeled as 6001e-0200e is unpertubed and has an upper state different from that of the discussed 6001e-1000e band. The upper levels of the 6001e-0200e and 6001e-1000e band are (16 0 17) upper and (16 0 19) at 9517.88 and 9606.33 cm^{-1}, respectively.

The second perturbed band is the 1004e-1000e band at 8603.7 cm^{-1} reaching the (18 0 4) upper state which is affected by couplings with two dark states: an intrapolyad anharmonic interaction with the (18 0 3) perturber state [(1802e) in normal mode notation] around *J*= 14 and an interpolyad Coriolis interaction with (17 1 10) [(3312e) in normal mode notation] around *J*= 34. The high *J* line positions (*J*

> 32) of the 1004e-1000e band were excluded from the fit of the spectroscopic constants. **Fig. 6** shows the impact of the perturbations on the 1004e-1000e band. The differences between the experimental and EH predicted values of the line positions included in the figure illustrate the improvements achieved by the non-polyad model of Ref. [1]. The (meas.-calc.) deviations are significantly reduced by the most recent non-polyad predictions [1].

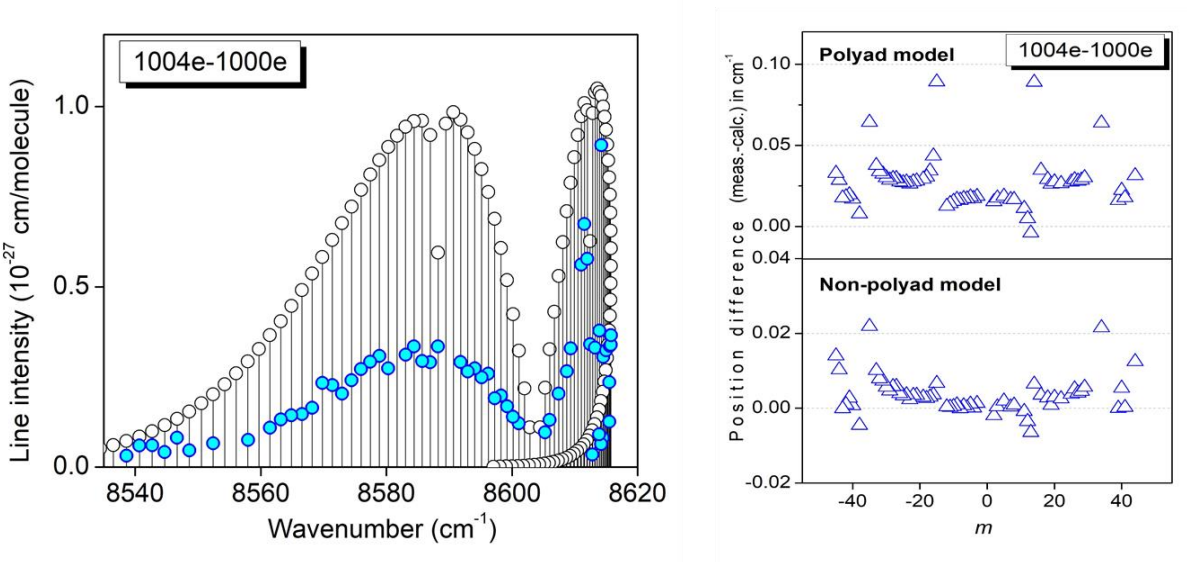

Fig. 6

The 1004e-1000e band at 8603.7 cm^{-1} reaching the (P l_2 i)= (18 0 4) state affected by two local parturbations around J= 14 and J= 34 (see **Table 3** and text).

Left panel: Comparison between the EH predictions (black circles) and the CRDS observations (cyan circles). Note the significant overestimation of the calculated intensities;

Right panels: Differences between the experimental and EH predicted values of the line positions (polyad model [27] and non-polyad EH model [1]).

4. Comparison to the HITRAN and HITEMP spectroscopic databases

Table 4

Comparison of the number of transitions and bands observed by CRDS with those provided by the HITRAN [26] and HITEMP [37] databases for the four N_2O isotopologues in the 8325-8622 cm^{-1} region.

Molecule	This work		HITRAN2016 [26]		HITEMP2019 [37]	
	Transitions	Bands	Transitions	Bands	Transitions	Bands
$^{14}N_2{}^{16}O$	2745	39			2433	31
$^{14}N^{15}N^{16}O$	299	3				
$^{15}N^{14}N^{16}O$	199	3				
$^{14}N_2{}^{18}O$	64	2	130	4	130	4
Total	3305	47	130	4	2563	35

The large amount of new experimental data obtained in this work gives us the possibility to check the quality of line parameters provided by different databases in the 8325-8622 cm^{-1} spectral region. Note that the Nitrous Oxide Spectroscopy Databank (NOSD) [36] constructed for $^{14}N_2{}^{16}O$ using

the effective operator approach does not extend beyond 8310 cm^{-1}. We thus focus on the N_2O line lists included in the HITRAN [26] and HITEMP [37] spectroscopic databases (see overview in **Fig. 7**). A comparative summary of the amount of transitions for the four N_2O isotopologues in the 8325-8622 cm^{-1} region is presented in **Table 4**.

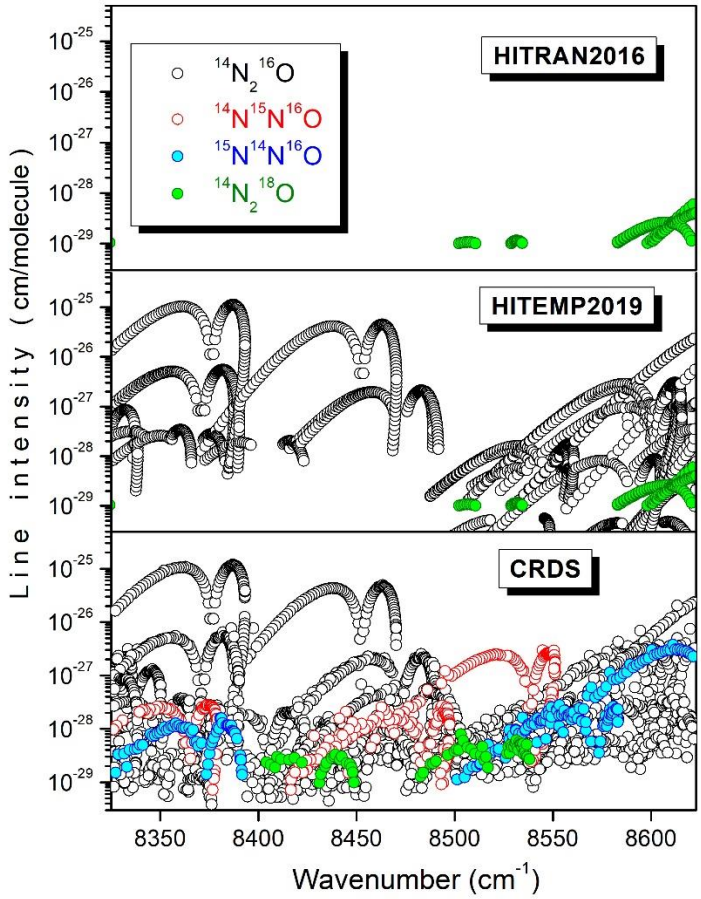

Fig.7
Overview comparison of the HITRAN2016 [26] and HITEMP2019 [37] line lists of N_2O in natural abundance to the CRDS measurements in the 8325-8622 cm^{-1} region.

In its present status, the N_2O line list in the HITRAN database [26] shows some deficiencies. In the near infrared, the HITRAN spectroscopic data relative to the main isotopologue is limited to FTS data below 7796 cm^{-1}, mostly from Toth database [3,4] and correspond to an intensity cut off of 2×10^{-25} cm/molecule at 296 K. The inclusion in the HITRAN dataset of the calculated line list of the fourth abundant isotopologue, $^{14}N_2{}^{18}O$, from Ref. [13] with an intensity cut off of 1×10^{-29} cm/molecule leads to an unusual situation: (i) in spite of a standard isotopic abundance of 0.001986 only, $^{14}N_2{}^{18}O$ is the isotopologue with largest amount of transitions in the present HITRAN2016 list, extending up to 10363 cm^{-1}, (ii) many bands of the main isotopologue which have been accurately measured in the literature (in particular by CRDS) and have intensity much higher than the $^{14}N_2{}^{18}O$ intensity cut off, are missing.

This situation is illustrated in the presently investigated region where the HITRAN line list includes only $^{14}N_2{}^{18}O$ transitions (they belong to the 7000-0000, 0004-0000, 0114-0110, 0513-0110 bands). The intensity of these calculated $^{14}N_2{}^{18}O$ lines range between 10^{-29} - 10^{-28} cm/molecule in our region (see **Fig. 8**) while transitions of $^{14}N_2{}^{16}O$ with line intensity larger than 10^{-25} cm/molecule are absent. Among the four HITRAN $^{14}N_2{}^{18}O$ bands, only the 7000-0000 band near 8521 cm^{-1} was measured in our CRDS spectra. The line position comparison (**Fig. 9**) shows a systematic overestimation of HITRAN position values by about 0.08 cm^{-1} for this band. Note that a second $^{14}N_2{}^{18}O$ band, the 6200-0000 band near 8429 cm^{-1}, with intensity slightly exceeding 10^{-29} cm/molecule was observed by CRDS but is missing in the HITRAN list. The $^{14}N^{15}N^{16}O$ and $^{15}N^{14}N^{16}O$ transitions are not provided in the HITEMP list in our region. Note that, in spite of an isotopic abundance of 3.641×10^{-3}, the $^{14}N^{15}N^{16}O$ isotopologue is the dominant absorber in the 8500-8550 cm^{-1} interval corresponding to the $4\nu_3$ band.

The HITEMP N_2O line list was recently constructed by merging three NOSD line lists at 296, 500 and 1000 K in order to allow to make the list applicable over the 296-1000 K range. The HITEMP list for nitrous oxide provides thus line positions and line intensities computed using the effective operator approach, and thus identical to the HITRAN list in the case of the $^{14}N_2{}^{18}O$ isotopologue.

In the case of $^{14}N_2{}^{16}O$, in our region, the HITEMP list includes 2433 transitions belonging to 31 bands. This is less than our CRDS observations (2745 transitions of 39 bands). The difference can be explained by the fact that *(i)* the ΔP= 15 bands are missing in HITEMP database because in absence of previous measurements of ΔP= 15 bands, the EDM parameters required to computed line intensities in the frame of the effective operator approach were missing, (ii) some EDM parameters of the ΔP= 14 and ΔP= 16 series were missing leading to underestimated values of the calculated intensities, below the intensity cut-off.

Overall, 19 bands in common could be compared. The overview comparisons are presented in **Fig. 8** and **Fig. 9** for line positions and line intensities, respectively. These figures correspond essentially to a subset of the whole set of bands compared in **Fig. 3** and **Fig. 4**, respectively. The (ν_{CRDS}-ν_{HITEMP}) deviations of $^{14}N_2{}^{16}O$ are limited to 0.12 cm^{-1} at maximum. Interestingly, $^{14}N_2{}^{16}O$ deviations are negative and positive below and above 8500 cm^{-1}.

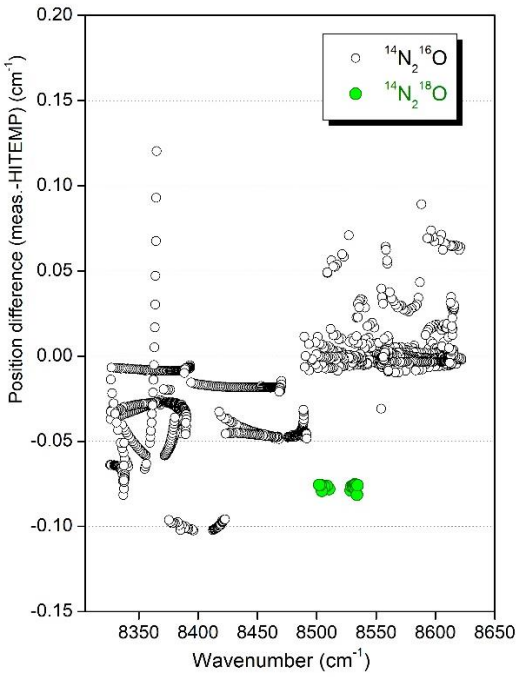

Fig. 8
Position difference the $^{14}N_2{}^{16}O$ and $^{14}N_2{}^{18}O$ measured line positions and those provided by HITEMP [37] database in the 8325-8622 cm^{-1} region, *versus* the wavenumber.

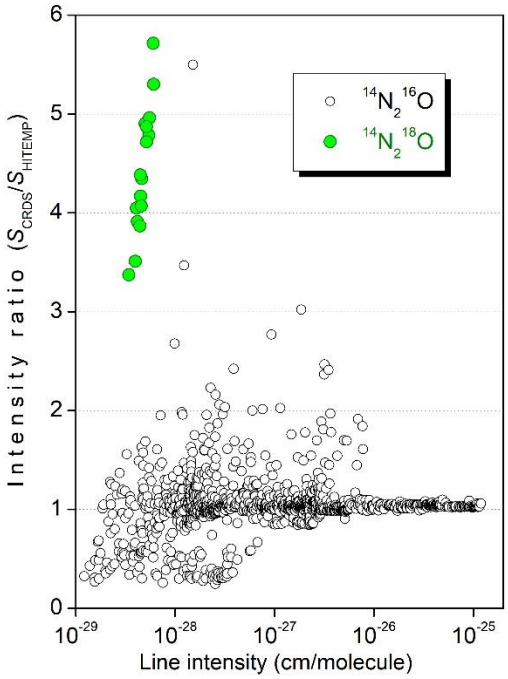

Fig. 9
Ratio of the $^{14}N_2{}^{16}O$ and $^{14}N_2{}^{18}O$ measured line intensities and those provided by HITEMP database [37] in the 8325-8622 cm^{-1} region, *versus* the CRDS line intensities.

5. Conclusion

The high sensitivity absorption spectrum of natural nitrous oxide has been recorded by CRDS in the 8325-8622 cm^{-1} range corresponding to a weak absorption region where previous measurements

were very limited. In particular, intensity information was totally missing. In total, 3307 lines were assigned to 47 bands of the $^{14}N_2{}^{16}O$, $^{14}N^{15}N^{16}O$, $^{15}N^{14}N^{16}O$, and $^{14}N_2{}^{18}O$ isotopologues. The weakest lines have an intensity of a few 10^{-30} cm/molecule at 296K. The line assignment was performed on the basis of predictions based on the effective operator approach. All identified bands belong to the Δ*P*= 14-16 series of transitions.

The observations in the considered 300 cm^{-1}-wide spectral interval have illustrated some deficiencies of the predicted N_2O line lists. All available line lists calculated within the effective operator approach show significant deviations compared to the observations in the region. For instance, the *rms* of the (meas.-calc.) deviations is 6×10^{-3} cm^{-1} for $^{14}N_2{}^{16}O$ *i.e.* about ten times larger than our claimed position accuracy (in the present work, a self-referenced frequency comb was used for the frequency scale calibration of the CRDS spectra). Larger deviations are noted for the minor isotopologues. As concerned line intensities, some Δ*P*= 14 and Δ*P*= 16 bands have their intensity calculated significantly too small while, in absence of previous observations and thus of corresponding fitted values of the effective moment parameters, intensity predictions of the Δ*P*= 15 bands were not possible.

As concerned spectroscopic databases in the considered region, the HITRAN2016 line list provides spectroscopic information for the only $^{14}N_2{}^{18}O$ isotopologue while absorption bands of the main species, $^{14}N_2{}^{16}O$, with 10^3 larger intensities, are missing. The HITEMP calculated line list is more complete but Δ*P*= 15 bands of $^{14}N_2{}^{16}O$ are absent. In addition, no data relative to $^{14}N^{15}N^{16}O$ and $^{15}N^{14}N^{16}O$ are provided while these two species have an important contribution in the region.

We hope that the present measurements will allow refining and extending the sets of effective dipole moment and effective Hamiltonian parameters of the respective N_2O isotopologues and will thus contribute to the improvement of the status of the N_2O line list in the HITRAN and HITEMP spectroscopic databases.

Acknowledgements

This work is jointly supported by CNRS (France) in the frame of the International Research Project “SAMIA” with IAO-Tomsk.

References

1. Tashkun SA. Global modeling of the $^{14}N_2{}^{16}O$ line positions within the framework of the non-polyad model of effective Hamiltonian. Journal of Quantitative Spectroscopy and Radiative Transfer 2019;231:88–101. https://doi.org/10.1016/j.jqsrt.2019.04.023.
2. Amiot C, Guelachvili G. Vibration-rotation bands of $^{14}N_2{}^{16}O$: 1.2 micron-3.3 micron region. J Mol Spectrosc 1974;51:475-91. https://doi.org/10.1016/0022-2852(74)90202-1.
3. Toth RA. Linelist of N_2O parameters from 500 to 7500 cm^{-1}. http://mark4sun.jpl.nasa.gov/n2o.html.
4. Toth RA. Line Positions and Strengths of N_2O between 3515 and 7800 cm^{-1}. Journal of Molecular Spectroscopy 1999;197:158–87. https://doi.org/10.1006/jmsp.1999.7907.
5. Bailly D, Pirali O, Vervloet M. $^{14}N_2{}^{16}O$ emission in the 4.5 μm region: high excitation of the bending mode transitions $v_1v_2v_3 \rightarrow v_1v^l_2$ (v_3-1) with $(2v_1+v_2)$= 5. J Mol Spectrosc 2003;222:180–90. https://doi.org/10.1016/S0022-2852(03)00179-6.
6. Daumont L, vander Auwera J, Teffo JL, Perevalov VI, Tashkun SA. Line intensity measurements in $^{14}N_2{}^{16}O$ and their treatment using the effective dipole moment approach. II. The 5400-11000 cm^{-1} region. Journal of Quantitative Spectroscopy and Radiative Transfer 2007;104:342–56. https://doi.org/10.1016/j.jqsrt.2006.09.004.
7. Wang L, Perevalov VI, Tashkun SA, Gao B, Hao LY, Hu SM. Fourier transform spectroscopy of N_2O weak overtone transitions in the 1–2 μm region. J Mol Spectrosc 2006:237;129-36. https://doi.org/10.1016/j.jms.2006.03.007.
8. Liu AW, Kassi S, Malara P, Romanini D, Perevalov VI, Tashkun SA, Hu SM, Campargue A. High sensitivity CW-cavity ring down spectroscopy of N_2O near 1.5 μm (I). J Mol Spectrosc 2007:244;33-47. https://doi.org/10.1016/j.jms.2006.03.007.
9. Liu AW, Kassi S, Perevalov VI, Tashkun SA, Campargue A. High sensitivity CW-cavity ring down spectroscopy of N_2O near 1.5 μm (II). J Mol Spectrosc 2007:244;48-62. https://doi.org/10.1016/j.jms.2007.05.010.
10. Lu Y, Mondelain D, Liu AW, Perevalov VI, Kassi S, Campargue A. High Sensitivity *CW*-Cavity Ring Down Spectroscopy of N_2O between 6950 and 7653 cm^{-1} (1.44-1.31 μm): I. Line positions. J Quant Spectrosc Radiat Transfer 2012;113:749-62. https://doi.org/10.1016/j.jqsrt.2012.03.005.
11. Karlovets EV, Lu Y, Mondelain D, Kassi S, Campargue, Tashkun SA, Perevalov VI, High sensitivity CW-Cavity Ring Down Spectroscopy of N_2O between 6950 and 7653 cm^{-1} (1.44–1.31 μm): II. Line intensities. J Quant Spectrosc Radiat Transfer 2013;117:81–7. https://doi.org/10.1016/j.jqsrt.2012.11.003.
12. Karlovets EV, Campargue A, Kassi S, Perevalov VI, Tashkun SA. High sensitivity Cavity Ring Down Spectroscopy of N_2O near 1.22 μm: (I) Rovibrational assignments and band-by-band analysis. J Quant Spectrosc Radiat Transfer 2016;169:36–48. https://doi.org/10.1016/j.jqsrt.2019.02.011.
13. Tashkun SA, Perevalov VI, Karlovets EV, Kassi S, Campargue A. High sensitivity Cavity Ring Down Spectroscopy of N_2O near 1.22 μm: (II) $^{14}N_2{}^{16}O$ line intensity modeling and global fit of $^{14}N_2{}^{18}O$ line positions. J Quant Spectrosc Radiat Transfer 2016;176:62–69. https://doi.org/10.1016/j.jqsrt.2016.02.020.
14. Bertin T, Mondelain D, Karlovets EV, Kassi S, Perevalov VI, Campargue A. High sensitivity cavity ring down spectroscopy of N_2O near 1.74 μm. J Quant Spec- trosc Radiat Transf 2019;229:40–9. https://doi.org/10.1016/j.jqsrt.2019.02.011.
15. Campargue A, Permogorov D, Bach M, Temsamani MA, Auwera J vander, Herman M, et al. Overtone spectroscopy in nitrous oxide. The Journal of Chemical Physics 1995;103:5931–8. https://doi.org/10.1063/1.470473.
16. Weirauch G, Kachanov AA, Campargue A, Bach M, Herman M, Vander Auwera J. Refined investigation of the overtone spectrum of nitrous oxide. Journal of Molecular Spectroscopy 2000;202:98–106. https://doi.org/10.1006/jmsp.2000.8114.
17. Herbin H, Picqué N, Guelachvili G, Sorokin E, Sorokina IT. N_2O weak lines observed between 3900 and 4050 cm^{-1} from long path absorption spectra. J Mol Spectrosc 2006;238:256–9. https://doi.org/10.1016/j.jms.2006.05.004.

18. Campargue A, Weirauch G, Tashkun SA, Perevalov VI, Teffo JL. Overtone spectroscopy of N_2O between 10000 and 12000 cm^{-1}: a test of the polyad approach. J Mol Spectrosc 2001;209:198–206. https://doi.org/10.1006/jmsp.2001.8414.
19. Bertseva E, Kachanov AA, Campargue A. Intracavity laser absorption spectroscopy of N_2O with a vertical external cavity surface emitting laser. Chem Phys Lett 2002;351:18–26. https://doi.org/10.1016/S0009-2614(01)01321-5.
20. Ding Y, Perevalov VI, Tashkun SA, Teffo JL, Hu S, Bertseva E, Campargue A. Weak overtone transitions of N2O around 1.05 μm by ICLAS-VECSEL. J Mol Spectrosc 2003;220:80–6. https://doi.org/10.1016/S0022-2852(03)00060-2.
21. Bertseva E, Campargue A, Perevalov VI, Tashkun SA. New observations of weak overtone transitions of N_2O by ICLAS-VeCSEL near 1.07 μm. J Mol Spectrosc 2004;226:196–200. https://doi.org/10.1016/j.jms.2004.03.021.
22. Liu AW, Kassi S, Perevalov VI, Tashkun SA, Campargue A. High sensitivity CW-cavity ring down spectroscopy of N_2O near 1.28 μm. J Mol Spectrosc 2011:267;191-9. https://doi:10.1016/j.jms.2011.03.025.
23. Liu AW, Kassi S, Perevalov VI, Hu SM, Campargue A. High sensitivity CW-cavity ring down spectroscopy of N_2O near 1.5 μm (III). J Mol Spectrosc 2009;254:20–7. https://doi.org/10.1016/j.jqsrt.2019.02.011.
24. Ni HY, Song KF, Perevalov VI, Tashkun SA, Liu AW, Wang L, et al. Fourier-transform spectroscopy of $^{14}N^{15}N^{16}O$ in the 3800-9000 cm^{-1} region and global modeling of its absorption spectrum. Journal of Molecular Spectroscopy 2008;248:41–60. https://doi.org/10.1016/j.jms.2007.11.011.
25. Song KF, Liu AW, Ni HY, Hu SM. Fourier-transform spectroscopy of $^{15}N^{14}N^{16}O$ in the 3500-9000 cm^{-1} region J Mol Spectrosc 2009;255:24–31. https://doi.org/10.1016/j.jms.2009.02.008
26. Gordon IE, Rothman LS, Hill C, Kochanov RV, Tan Y, Bernath PF, et al. The HITRAN2016 molecular spectroscopic database. Journal of Quantitative Spectroscopy and Radiative Transfer 2017;203:3–69. https://doi.org/10.1016/j.jqsrt.2017.06.038.
27. Perevalov VI, Tashkun SA, Kochanov RV, Liu AW, Campargue A. Global modeling of the $^{14}N_2{}^{16}O$ line positions within the framework of the polyad model of effective Hamiltonian. Journal of Quantitative Spectroscopy and Radiative Transfer 2012;113:1004–12. https://doi.org/10.1016/j.jqsrt.2011.12.008.
28. Tashkun SA, Perevalov VI, Kochanov RV, Liu AW, Hu SM. Global fittings of $^{14}N^{15}N^{16}O$ and $^{15}N^{14}N^{16}O$ vibrational-rotational line positions using the effective Hamiltonian approach. Journal of Quantitative Spectroscopy and Radiative Transfer 2010;111:1089–105. https://doi.org/10.1016/j.jqsrt.2010.01.010.
29. Mondelain D, Kassi S, Sala T, Romanini D, Marangoni M, Campargue A. Sub-MHz accuracy measurement of the S(2) 2–0 transition frequency of D_2 by comb-assisted cavity ring down spectroscopy. J Mol Spectrosc 2016;326:5–8. https://doi.org/10.1016/j.jms.2016.02.008.
30. Kassi S, Campargue A. Cavity Ring Down Spectroscopy with 5×10^{-13} cm^{-1} sensitivity. J Chem Phys 2012;137:234201. https://doi.org/10.1063/1.4769974.
31. Konefał M, Mondelain D, Kassi S, Campargue A. High sensitivity spectroscopy of the O_2 band at 1.27 μm: (I) pure O_2 line parameters above 7920 cm^{-1}. J Quant Spectrosc Radiat Transfer 2020;241:106653. https://doi.org/10.1016/j.jqsrt.2019.106653.
32. Mondelain D, Mikhailenko SN, Karlovets EV, Béguier S, Kassi S, Campargue A. Comb-Assisted Cavity Ring Down Spectroscopy of ^{17}O enriched water between 7443 and 7921 cm^{-1}. J Quant Spectrosc Radiat Transfer 2017;203:206–12. https://doi.org/10.1016/j.jqsrt.2017.03.029.
33. Kassi S, Stoltmann T, Casado M, Daëron M, Campargue A. Lamb dip CRDS of highly saturated transitions of water near 1.4 μm. J Chem Phys 2018;148:054201. https://doi.org/10.1063/1.5010957.
34. Karlovets EV, Perevalov VI. The influence of isotopic substitution on the effective dipole moment parameters of CO_2 molecule. Optics and Spectroscopy 2015;119:16–21. https://doi.org/10.1134/S0030400X15070139.

35. Tashkun SA, Perevalov VI, Teffo JL, Tyuterev VI.G. Global fit of $^{12}C^{16}O_2$ vibrational rotational line intensities using the effective operator approach. Journal of Applied Physics 1999;62:571–98. https://doi.org/10.1063/1.1658372.
36. Tashkun SA, Perevalov VI, Lavrentieva NN. NOSD-1000, the high-temperature nitrous oxide spectroscopic databank. Journal of Quantitative Spectroscopy and Radiative Transfer 2016;177:43–8. https://doi.org/10.1016/j.jqsrt.2015.11.014.
37. Hargreaves RJ, Gordon IE, Rothman LS, Tashkun SA, Perevalov VI, Lukashevskaya AA, et al. Spectroscopic line parameters of NO, NO_2, and N_2O for the HITEMP database. Journal of Quantitative Spectroscopy and Radiative Transfer 2019;232:35–53. https://doi.org/10.1016/j.jqsrt.2019.04.040.

Table 2

Spectroscopic parameters (in cm^{-1}) for the different bands of N_2O isotopologues assigned in the CRDS spectrum between 8325 and 8622 cm^{-1}. The bands are ordered in increasing order of the band center. The lower state constants were constrained to the values provided in Refs. [3,4].

Band											
$v_1\ v_2 l_2 v_3$ [a]	$(P\ l_2\ i)$ [b]	ΔG_v [c]	G_v	B_v	$D_v \times 10^7$	$H_v \times 10^{12}$	RMS [d]	N_{fit}/N_{obs} [e]	$J_{max\ P/Q/R}$ [f]	ΔP [g]	Note [h]
$^{14}N_2{}^{16}O$											
6111e-1110e	(17 1 17)- (3 1 2)	8316.60519(95) [i]						0/7	R24	14	
6111f-1110f		8316.60546(49) [i]						0/10	R24	14	
0(10)00e-0000e	(14 0 13)-(0 0 1)	8319.79374(56)	8319.79374(56)	0.4178021(34)	12.881(52)	157.5(22)	0.60	25/25	R37	14	
6001e-1000e	(16 0 19)-(2 0 2)	8321.42943(61)	9606.33277(61)	0.4072716(33)	1.847(21)	16.19(35)	0.68	15/37	R57	14	1
1113e-0000e	(15 1 3)-(0 0 1)	8335.796710(99)	8335.796710(99)	0.40719706(21)	1.70927(76)		0.44	56/58	P10/R56	15	
1113f-0000e		8335.79641(11)	8335.79641(11)	0.40804104(74)	1.6908(90)		0.28	27/28	Q29	15	
6111e-0310e	(17 1 17)-(3 1 1)	8338.13194(70)	10087.19717(70)	0.4087204(44)	2.373(50)		0.94	14/16	P12/R28	14	
6111f-0310f		8338.13332(78)	10087.19847(78)	0.4113325(38)	2.432(36)		0.91	10/14	P12/R31	14	
6001e-0200e	(16 0 17)-(2 0 1)	8349.74209(15)	9517.87439(15)	0.4094555(23)	3.464(75)	201.3(61)	0.45	41/44	P22/R28	14	
5331e-0330e	(17 3 27)-(3 3 2)	8358.12762(21)	10125.03999(21)	0.41148294(88)	1.5180(68)		0.46	31/35	P29/R35	14	2
5331f-0330f		8358.12798(24)	10125.04022(24)	0.4114837(10)	1.5108(78)		0.53	31/35	P29/R35	14	
5221e-0220e	(16 2 27)-(2 2 2)	8365.17471(16)	9542.91938(16)	0.4108188(13)	0.995(21)		0.47	38/44	P27/R25	14	2
5221e-0220f								6/6	Q10	14	
5221f-0220f		8365.17463(14)	9542.91930(14)	0.4108235(12)	1.751(19)		0.43	37/44	P27/R25	14	
5221f-0220e								6/6	Q10	14	
5111e-0110e	(15 1 12)-(1 1 1)	8370.995106(56)	8959.762976(56)	0.40897235(21)	1.8035(18)	1.428(38)	0.29	78/78	P37/R59	14	
5111e-0110f								17/19	Q24	14	
5111f-0110f		8370.994969(80)	8959.762839(80)	0.41101680(35)	1.7813(34)	2.993(80)	0.40	79/80	P38/R55	14	
5111f-0110e								21/22	Q28	14	
5001e-0000e	(14 0 14)-(0 0 1)	8376.349787(69)	8376.349787(69)	0.40893705(22)	2.1485(17)	5.074(31)	0.34	99/99	P40/R61	14	

3601e-1000e	(16 0 20)-(2 0 2)	8405.17879(13)	9690.08214(13)	0.40871176(75)	-0.2739(98)	10.26(33)	0.51	69/72	P43/R45	14	
3421e-0000e	(14 2 46)-(0 0 1)	8414.80509(26)	8414.80509(26)	0.41121716(55)	1.3412(31)	-6.151(48)	0.49	63/69	P57/R64	14	
3711e-1110e	(17 1 20)-(3 1 2)	8421.41763(52)	10301.68337(52)	0.4077371(38)	0.785(52)		0.74	17/21	P26/R25	14	
3711f-1110f		8421.41692(81)	10301.68266(81)	0.4102881(53)	0.243(74)		0.88	20/29	P26/R25	14	
0712f-0000e	(15 1 5)-(0 0 1)	8425.02370(23)	8425.02370(23)	0.41365577(78)	2.7183(52)		0.55	25/30	Q42	15	
0712e-0000e		8425.02415(27)	8425.02415(27)	0.41147138(98)	2.4429(62)		0.81	38/42	P23/R40	15	
0(16)00e-0200e	(16 0 32)-(2 0 1)	8430.96855(77)	9599.10085(77)	0.4155477(54)	12.015(77)		0.82	16/26	P26/R23	14	
0(16)20e-0220e	(16 2 27)-(2 2 2)	8432.12679(84)	9609.87146(84)	0.415755(48)	-7.19(84)		0.56	7/13	P28/R29	14	
0(16)20f-0220f		8432.12714(61)	9609.87181(61)	0.4158163(25)	3.718(20)		0.47	9/15	P28/R32	14	
3401e-0000e	(14 0 15)-(0 0 1)	8452.635571(90)	8452.635571(90)	0.40903776(24)	0.3989(14)	6.565(23)	0.46	102/109	P65/R68	14	
6310e-0110e	(15 1 15)-(1 1 1)	8452.87707(17)	9041.64494(17)	0.41353353(99)	3.7686(93)	-	0.50	33/37	P26/R34	14	
6310f-0110f		8452.87647(24)	9041.64434(24)	0.4176904(15)	4.323(22)	-8.10(87)	0.69	51/52	P43/R36	14	
3511e-0110e	(15 1 16)-(1 1 1)	8472.57405(11)	9061.34192(11)	0.40866282(43)	1.0799(38)	3.050(89)	0.51	88/95	P55/R55	14	
3511e-0110f								11/12	Q13	14	
3511f-0110f		8472.57389(77)	9061.341763(77)	0.41068060(36)	0.5947(38)	3.37(10)	0.34	79/85	P54/R53	14	
3511f-0110e								11/13	Q15	14	
6200e-0000e	(14 0 17)-(0 0 1)	8475.72562(15)	8475.72562(15	0.41549050(60)	8.3324(60)	63.59(16)	0.54	79/84	P45/R51	14	
3621e-0220e	(16 2 35)-(2 2 2)	8484.52563(28)	9662.27030(28)	0.4103132(21)	1.814(38)	-6.6(17)	0.72	37/46	P41/R38	14	
3621e-0220f								4/6	Q11	14	
3621f-0220f		8484.52643(32)	9662.27110(32)	0.4102732(36)	-1.468(64)		0.70	21/24	P24/R22	14	
3621f-0220e								4/6	Q11	14	
0204e-1000e	(18 0 1)-(2 0 2)	8485.73231(26)	9770.63565 (26)	0.4064288(11)	2.4996(84)		0.77	38/44	P36/R36	16	
3601e-0200e	(16 0 20)-(2 0 1)	8521.95155(21)	9690.08385(21)	0.40869850(97)	-0.5001(82)		0.57	33/49	P36/R37	14	
0334e-0330e	(19 3 2)-(3 3 2)	8545.04804(16)	10311.96042(16)	0.40731223(50)	1.6424(26)		0.68	58/67	P47/R41	16	2
0334e-0330f								8/11	Q21	16	
0334f-0330f		8545.04910(18)	10311.96134(18)	0.40730875(57)	1.5921(33)		0.66	53/66	P46/R41	16	
0334f-0330e								6/12	Q21	16	

1114e-1110e	(19 1 4)-(3 1 2)	8547.66748(36)	10427.93322(36)	0.4037404(19)	1.524(16)		0.50	9/21	P36/R25	16	
1114f-1110f		8547.66618(61)	10427.93192(61)	0.4045852(23)	1.670(19)		0.64	10/15	P31/R33	16	
0314e-0310e	(19 1 1)-(3 1 1)	8547.97543(21)	10297.04066(21)	0.40629281(64)	2.0941(34)		0.73	43/51	P48/R25	16	
0314f-0310f		8547.97460(14)	10297.03975(14)	0.40770388(42)	2.2605(22)		0.50	50/58	P49/R38	16	
3112e-0000e	(15 1 8)-(0 0 1)	8559.18244(35)	8559.18244(35)	0.4092951(25)	2.302(42)	35.5(20)	0.77	38/46	P32/R37	15	
3112f-0000e		8559.18456(36)	8559.18456(36)	0.4109122(23)	1.499(27)		0.63	19/20	Q29	15	
7200e-0200e	(16 0 21)-(2 0 1)	8578.42447(76)	9746.55677(76)	0.4132943(63)	8.50(13)	115.4(78)	0.64	17/22	P33/R26	14	
8000e-1000e	(16 0 22)-(2 0 2)	8589.39250(33)	9874.29584(33)	0.4108183(16)	4.527(16)		0.69	25/32	P34/R30	14	
0005e-0001e	(20 0 1)-(4 0 1)	8591.48559(53)	10815.24236(53)	0.4044182(49)	19.88(12)	521.3(82)	0.70	23/27	P32/R26	16	
7110e-0110e	(15 1 17)-(1 1 1)	8596.92927(20)	9185.69714(20)	0.4116082(11)	3.089(13)	7.86(43)	0.55	48/53	P47/R44	14	
7110f-0110f		8596.92911(16)	9185.69698(16)	0.41518951(46)	3.2864(24)		0.56	48/54	P48/R38	14	
0224e-0220e	(18 2 2)-(2 2 2)	8600.95914(15)	9778.70381(15)	0.40661236(76)	1.1636(66)	-3.70(15)	0.60	55/84	P46/R54	16	3
0224e-0220f								10/14	Q18	16	
0224f-0220f		8600.95966(16)	9778.70433(16)	0.40661199(68)	1.8247(57)	0.31(12)	0.66	58/73	P59/R29	16	
0224f-0220e								7/12	Q16	16	
0204e-0200e	(18 0 1)-(2 0 1)	8602.50293(10)	9770.63523(10)	0.40643300(44)	2.5877(41)	4.392(98)	0.44	77/81	P57/R29	16	
1004e-1000e	(18 0 4)-(2 0 2)	8603.66354(22)	9888.56688(22)	0.4033323(13)	1.562(14)	-	0.66	40/60	P45/R43	16	4
6200e-0000e	(14 0 17)-(0 0 1)	8612.948127(93)	8612.948127(93)	0.41313128(54)	5.0256(65)	21.07(20)	0.35	56/57	P49/R11	14	
0004e-0000e	(16 0 1)-(0 0 1)	8714.1688(39)	8714.1688(39)	0.4051668(17)	1.7416(18)		0.40	15/16	P78	16	
0623e-0220e	(18 2 4)-(2 2 2)	8634.70603(97)	9812.45070(97)	0.4116852(31)	-0.513(18)		0.75	10/14	P39	16	
0623f-0220f		8634.7057(24)	9812.4504(24)	0.4116653(99)	2.907(93)		0.93	8/9	P30	16	
0603e-0200e	(18 0 2)-(2 0 1)	8637.6421(18)	9805.7744(18)	0.4114861(71)	6.304(76)	47.9(24)	0.68	15/18	P43	16	
0114e-0110e	(17 1 1)-(1 1 1)	8657.31616(28)	9246.08403(28)	0.40553278(27)	1.78191(56)		0.26	33/36	P67	16	
0114f-0110f		8657.31729(51)	9246.08516(51)	0.40627830(52)	1.8080(12)		0.41	30/30	P62	16	
$^{14}N^{15}N^{16}O$ isotopologue											
5001e-0000e	(14 0 14)-(0 0 1)	8364.70516(26)	8364.70516(26)	0.4071009(12)	1.261(14)	5.88(39)	0.61	46/57	P32/R49	14	
0114e-0110e	(17 1 1)-(1 1 1)	8484.55859(19)	9059.99224(19)	0.40592363(45)	1.7548(21)		0.62	49/72	P47/R48	16	5

0114f-0110f		8484.55857(26)	9059.99222(26)	0.40568004(60)	1.7738(27)		0.76	45/73	P47/R49	16	
0004e-0000e	(16 0 1)-(0 0 1)	8538.510472(78)	8538.510472(78)	0.40562357(14)	1.74262(43)		0.43	93/97	P58/R60	16	
$^{15}N^{14}N^{16}O$											
3401e-0000e	(14 0 15)-(0 0 1)	8372.78730(14)	8372.78730(14)	0.39620588(50)	1.141(32)		0.55	54/60	P40/R42	14	
0114e-0110e	(17 1 1)-(1 1 1)	8571.99343(23)	9157.30555(23)	0.39176315(60)	1.6458(29)		0.63	34/46	P49/R21	16	6
0114f-0110f		8571.99347(28)	9157.30559(28)	0.39247119(78)	1.7158(39)		0.68	31/46	P47/R21	16	
0004e-0000e	(16 0 1)-(0 0 1)	8628.68395(16)	8628.68395(16)	0.39140762(30)	1.6493(10)		0.47	43/47	P56	16	
$^{14}N_2{}^{18}O$											
6200e-0000e	(14 0 17)-(0 0 1)	8428.79746(27)	8428.79746 (27)	0.3893979(12)	3.1544 (95)		0.57	20/22	P26/R35	14	
7000e-0000e	(14 0 18)-(0 0 1)	8520.97376(36)	8520.97376(36)	0.3876247(16)	1.147(14)		0.78	31/42	P36/R32	14	

Notes

The confidence interval (1SD) is in the units of the last quoted digit.

[a] $v_1\ v_2 l_2 v_3$ correspond to the maximum value of the modulo of the expansion coefficients of the eigenfunction. V_2 is given between parenthesis when it is larger than 10,

[b] Cluster labelling notation: (P=2V_1+V_2+4V_3, l_2, i), i is the order number within the cluster increasing with the energy,

[c] $\Delta G_v = G_v' - G_v''$ is the band center,

[d] Root Mean Square of the (Obs.-Calc.) differences of the position values (in 10^{-3} cm^{-1} unit),

[e] N_{fit} is the total number of transitions included in the fit; N_{obs} is the total number of measured transitions of the considered band,

[f] Observed branch with the maximum value of the total angular momentum quantum number of the input data,

[g] $\Delta P = P' - P''$, where P' and P'' are the upper and lower polyads,

[h] Notes:

1. This band is affected by a local perturbation at J= 29 (see Table 3);
2. The *e* and *f* components are blended for all lines;
3. The *e* and *f* components are blended for *P*-branch (J=3-42,44,46), for *R*-branch (J=4-29), and for *Q*-branch (J=2-16). Most of the lines were excluded from the fit;
4. This band is affected by two local perturbations at J= 14 and J= 34 (see Table 3);
5. The *e* and *f* components are blended for *P*-branch (J=2-4) and for *R*-branch (J= 1-8,17,18,20,22-28). These lines were excluded from the fit; 6. The *e* and *f* components are blended for *P*-branch (J=3) and for *R*-branch (J= 1-9). These lines were excluded from the fit.

[i] The band center provided by the global effective Hamiltonian.

Fig. 1

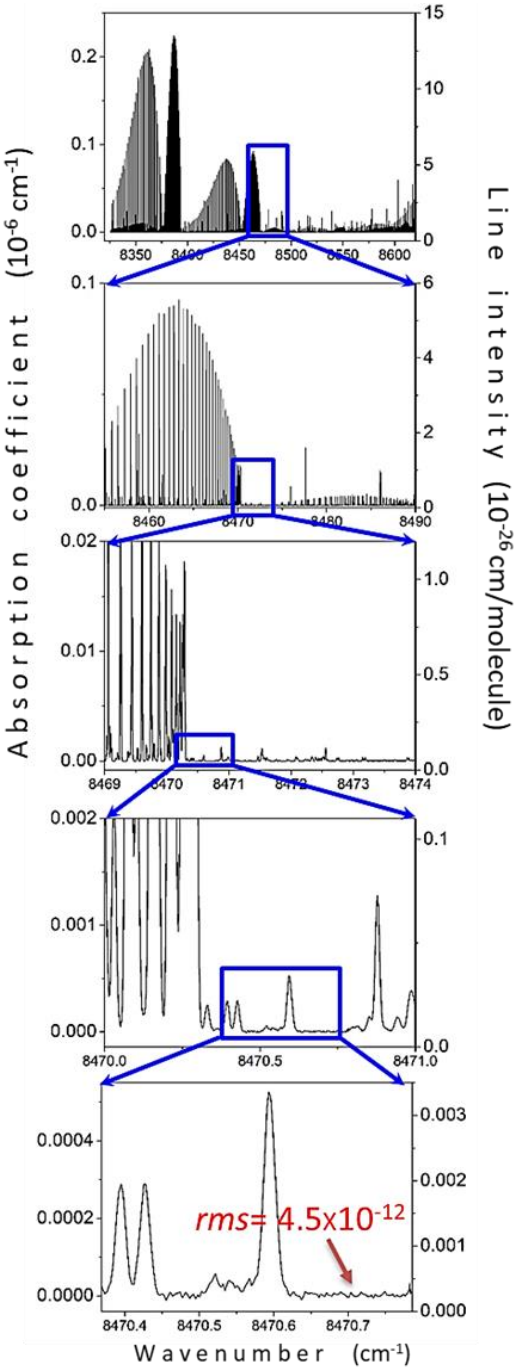

Fig. 2

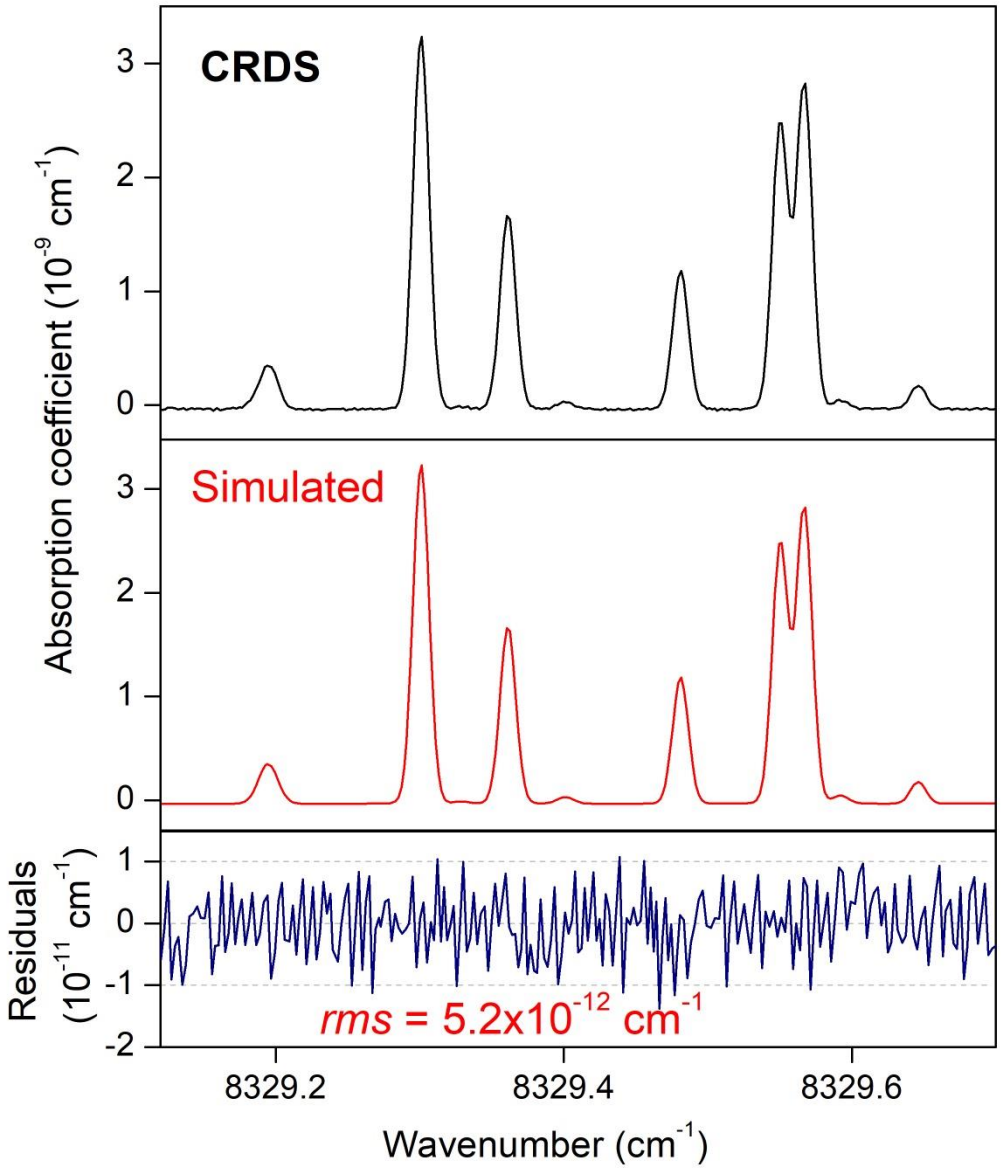
CRDS
Simulated
Absorption coefficient (10^{-9} cm^{-1})
Residuals (10^{-11} cm^{-1})
rms = 5.2x10^{-12} cm^{-1}
Wavenumber (cm^{-1})
8329.2
8329.4
8329.6

Fig. 3

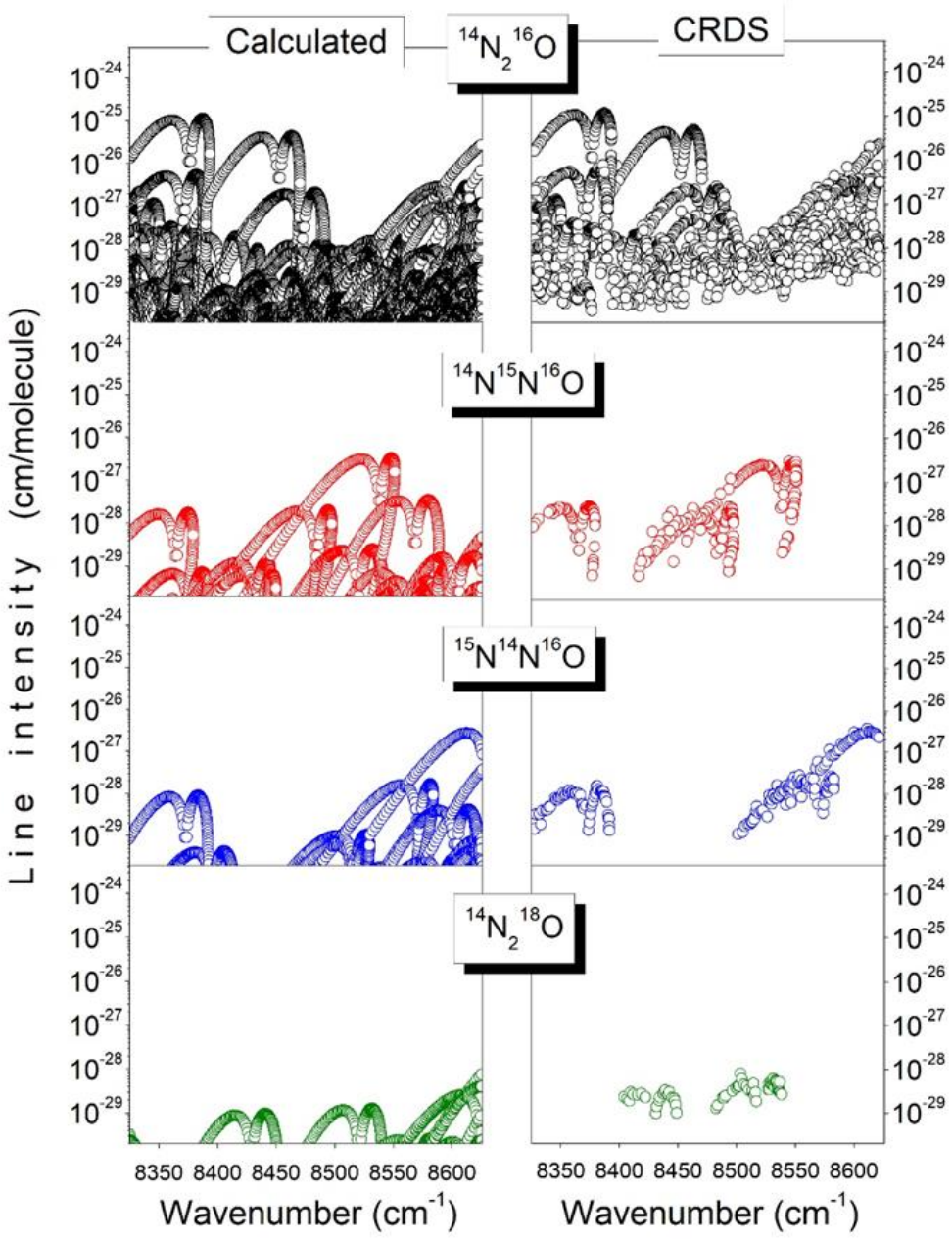
Calculated
CRDS
$^{14}N_2{}^{16}O$
$^{14}N^{15}N^{16}O$
$^{15}N^{14}N^{16}O$
$^{14}N_2{}^{18}O$
Line intensity (cm/molecule)
10^{-24}
10^{-25}
10^{-26}
10^{-27}
10^{-28}
10^{-29}
8350 8400 8450 8500 8550 8600
Wavenumber (cm^{-1})

Fig. 4

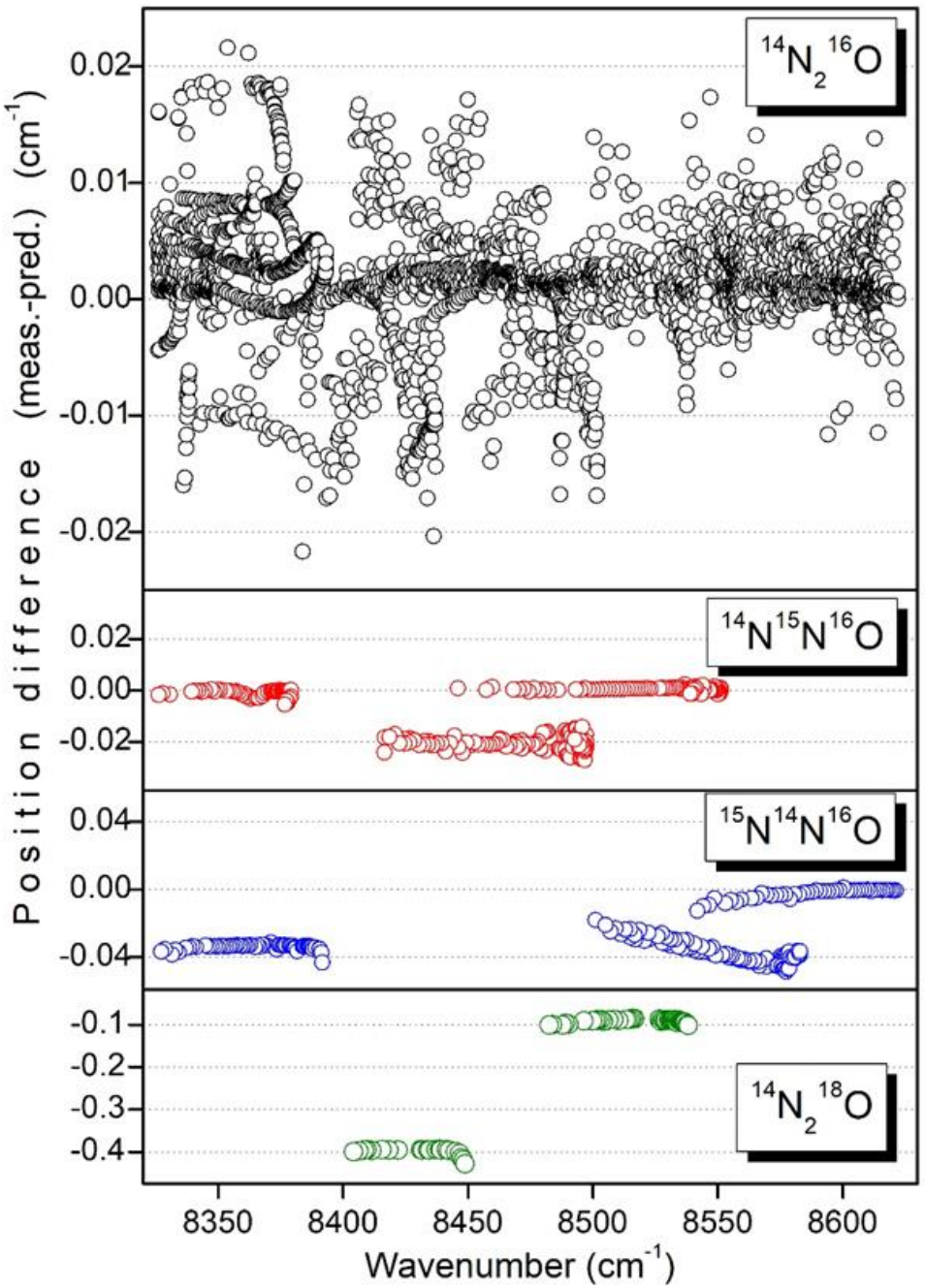
$^{14}N_2{}^{16}O$
$^{14}N^{15}N^{16}O$
$^{15}N^{14}N^{16}O$
$^{14}N_2{}^{18}O$
Position difference (meas.-pred.) (cm^{-1})
Wavenumber (cm^{-1})
0.02
0.01
0.00
-0.01
-0.02
0.04
-0.04
-0.1
-0.2
-0.3
-0.4
8350
8400
8450
8500
8550
8600

Fig. 5

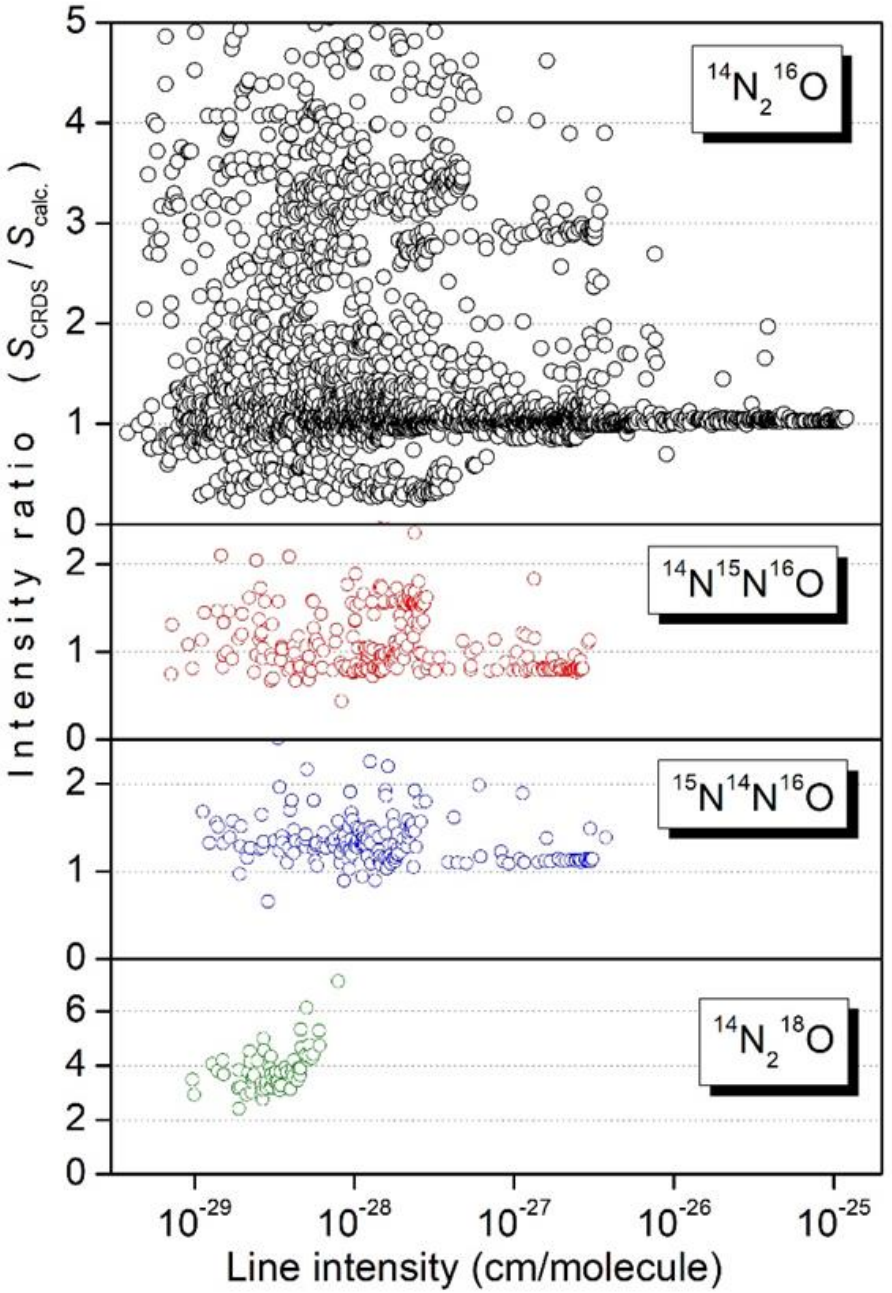
Intensity ratio (S_{CRDS} / $S_{calc.}$)
$^{14}N_2{}^{16}O$
$^{14}N^{15}N^{16}O$
$^{15}N^{14}N^{16}O$
$^{14}N_2{}^{18}O$
Line intensity (cm/molecule)

Fig. 6

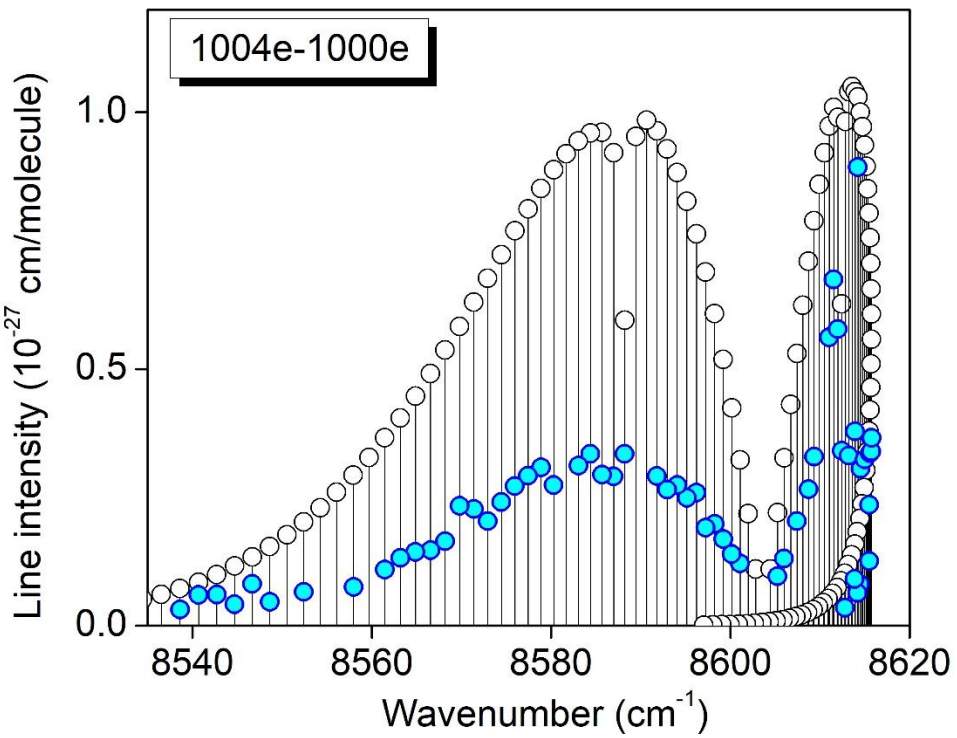
1004e-1000e
Line intensity (10^{-27} cm/molecule)
1.0
0.5
0.0
8540
8560
8580
8600
8620
Wavenumber (cm^{-1})

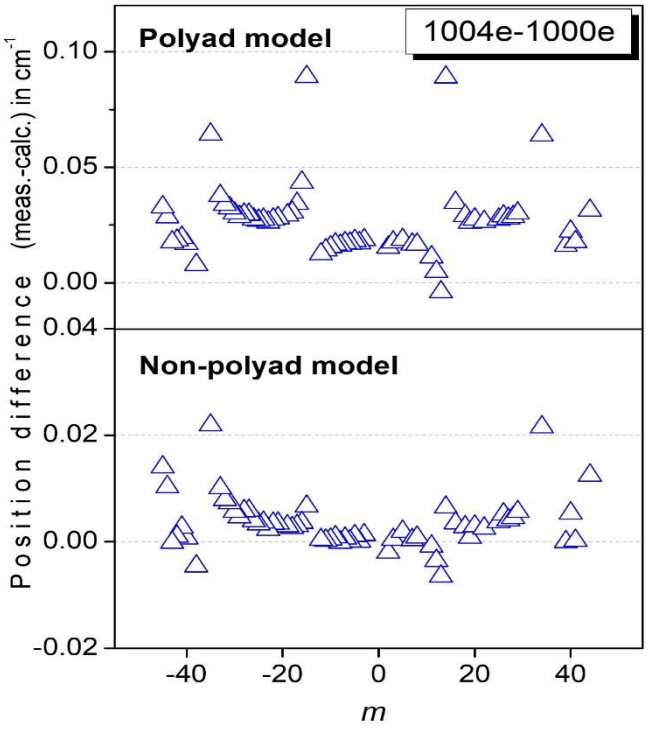
Polyad model
1004e-1000e
Non-polyad model
Position difference (meas.-calc.) in cm^{-1}
0.10
0.05
0.00
0.04
0.02
0.00
-0.02
-40
-20
0
20
40
m

Fig. 7

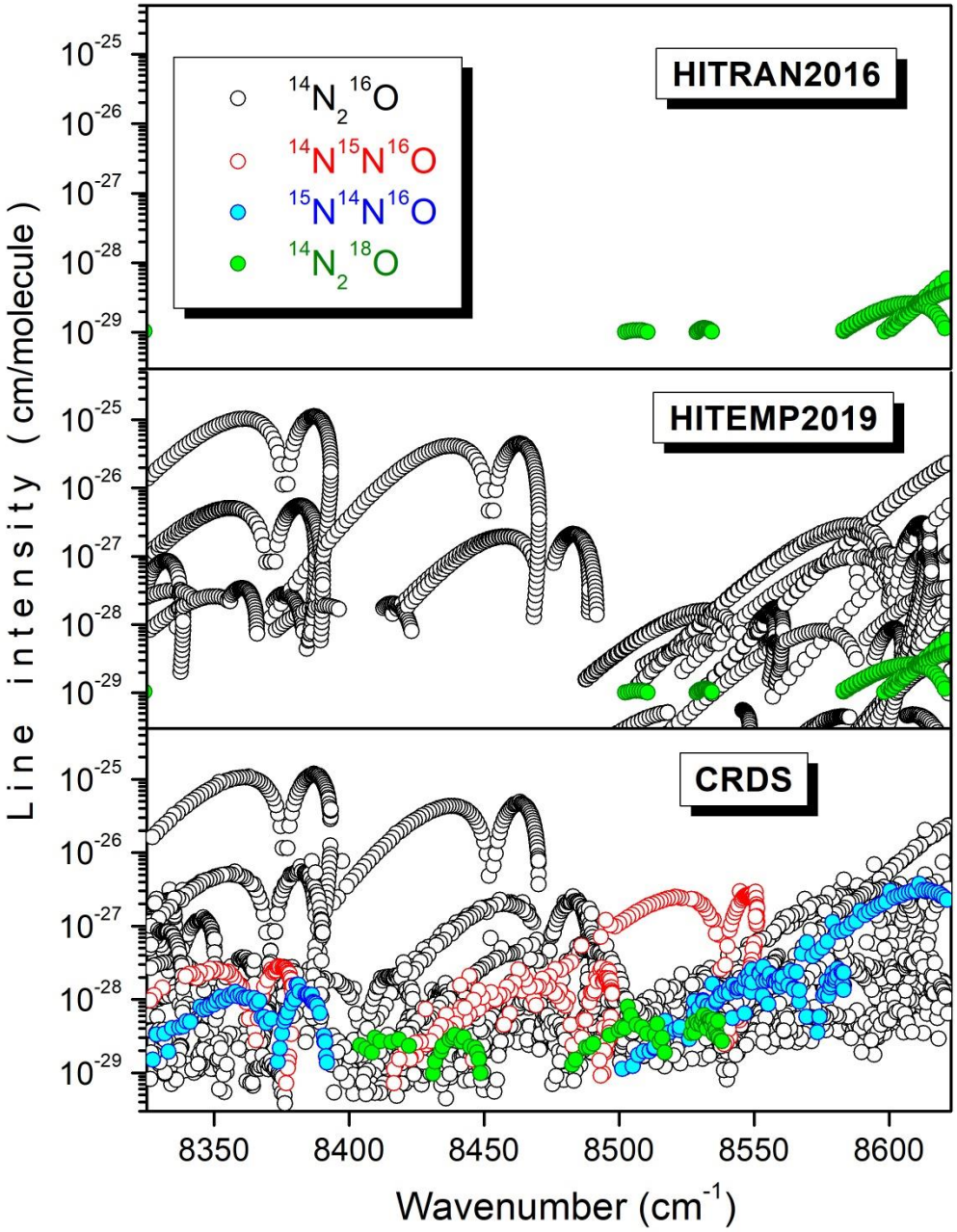
HITRAN2016
HITEMP2019
CRDS
$^{14}N_2{}^{16}O$
$^{14}N^{15}N^{16}O$
$^{15}N^{14}N^{16}O$
$^{14}N_2{}^{18}O$
Line intensity (cm/molecule)
10^{-25}
10^{-26}
10^{-27}
10^{-28}
10^{-29}
8350
8400
8450
8500
8550
8600
Wavenumber (cm^{-1})

Fig. 8

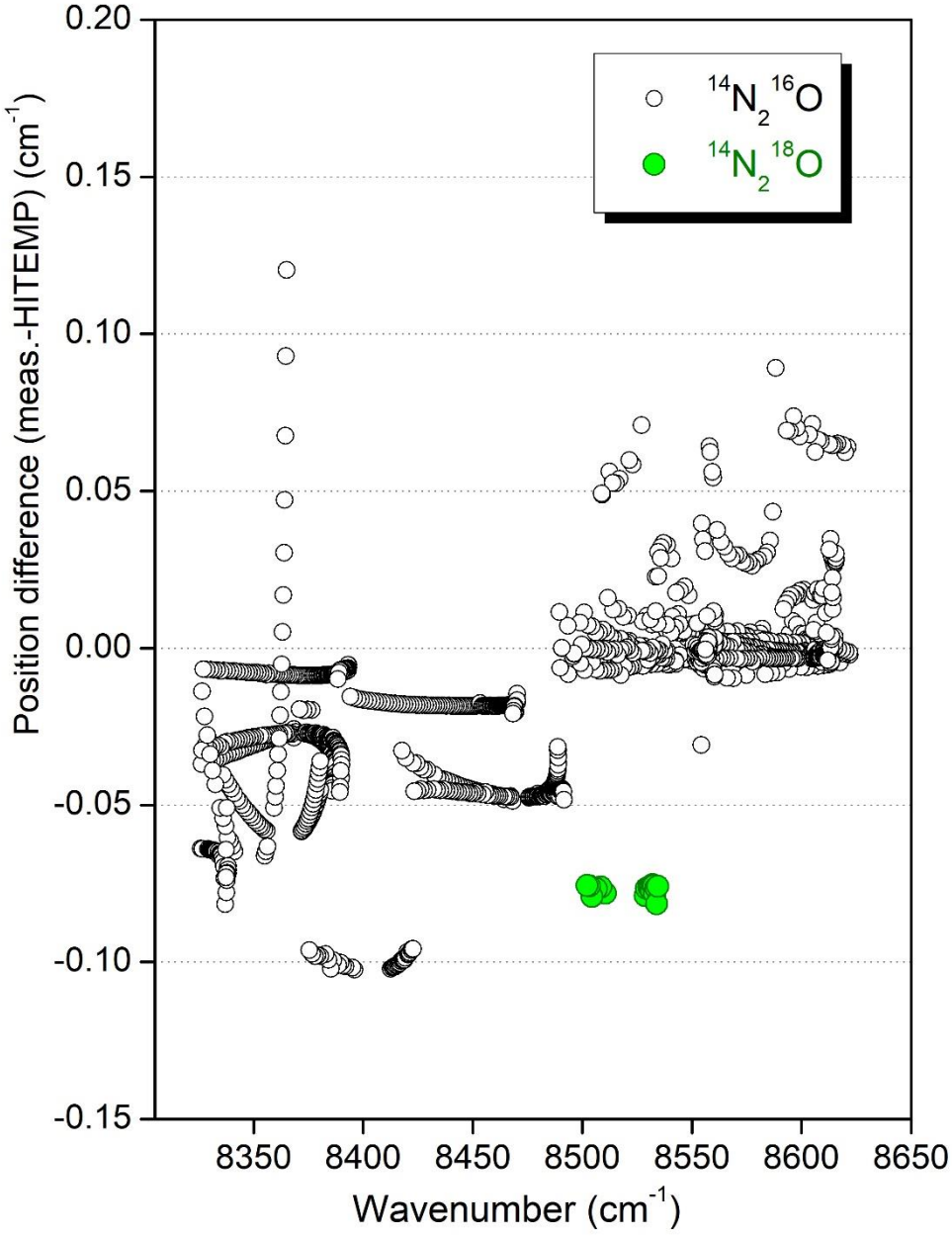
0.20
0.15
0.10
0.05
0.00
-0.05
-0.10
-0.15
Position difference (meas.-HITEMP) (cm-1)
8350
8400
8450
8500
8550
8600
8650
Wavenumber (cm-1)
14N2 16O
14N2 18O

Fig. 9

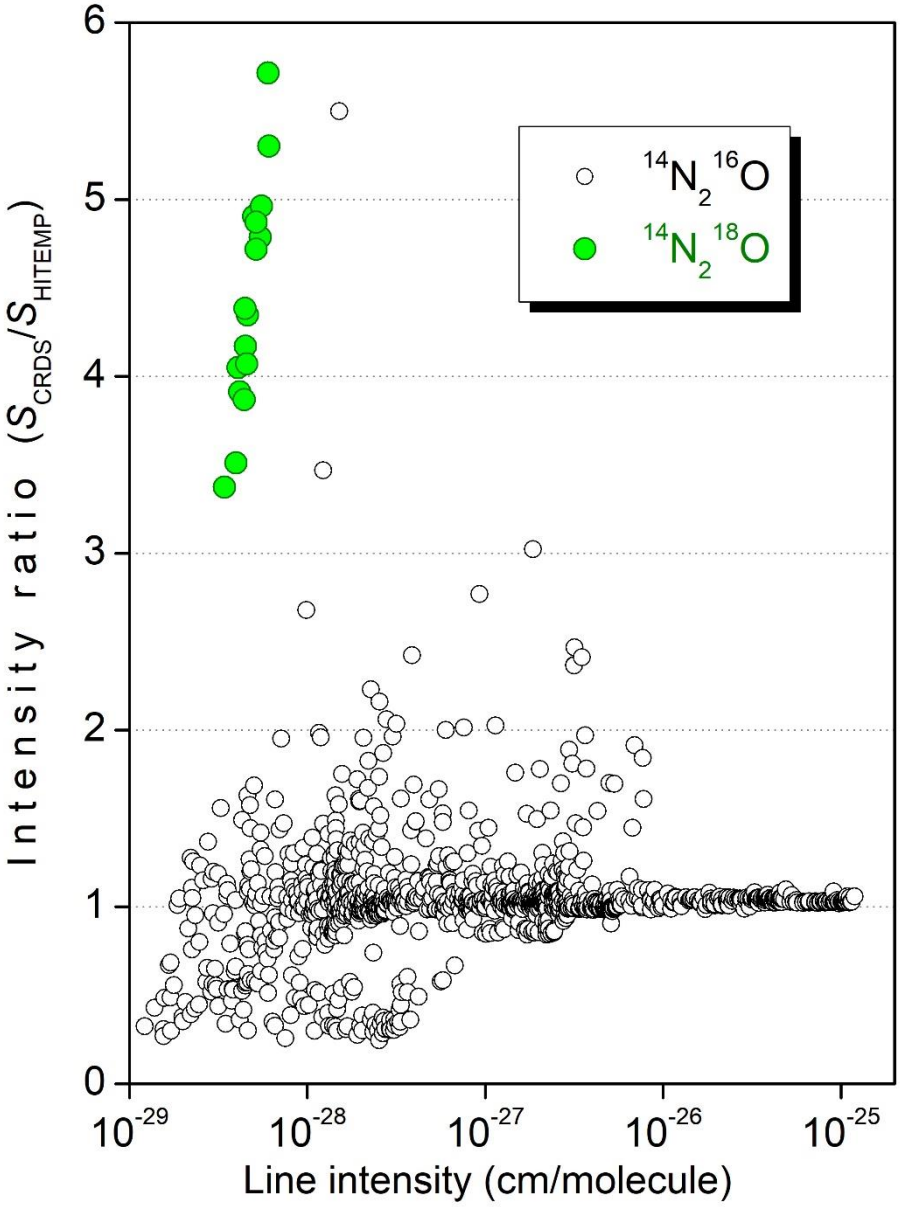
Intensity ratio (S_{CRDS}/S_{HITEMP})
Line intensity (cm/molecule)
$^{14}N_2{}^{16}O$
$^{14}N_2{}^{18}O$
0
1
2
3
4
5
6
10^{-29}
10^{-28}
10^{-27}
10^{-26}
10^{-25}

Conflict of Interest

The authors declare that they have no known competing financial interests or personal relationships that could have appeared to influence the work reported in this paper.

E.V. Karlovets: Data curation, Writing. **S.Kassi:** Investigation. **S.A.Tashkun:** Investigation. **A. Campargue:** Data analysis, Writing the paper.